Photoelastic Stress Analysis of Polyethylene Terephthalate

Gabriela dos Santos Kotila

Degree Thesis

Materials Processing Technology

2018

DEGREE THESIS	
Arcada	
Degree Programme:	Materials Processing Technology
Identification number:	6220
Author:	Gabriela dos Santos Kotila
Title:	Photoelastic Stress Analysis of Polyethylene Terephthalate
Supervisor (Arcada):	Rene Herrmann
Commissioned by:	Mathew Vihtonen

Abstract:

Photoelasticity is an experimental stress/strain-analysis method. This technique is based on the photoelastic effect which is a change in the optical indicatrix with mechanical stress. A polariscope is an instrument used for photoelastic stress analysis. In the research performed to write this paper a plane polariscope was used to analyse injection moulded PET samples. The main objective of this work is to investigate the internal stress in PET caused due to thermal contraction (shrinkage) during processing. A new method of data analysis is used where pictures are captured from the samples and then the data from the image is extracted to create a pixel count-intensity graph. Different loads were applied to the samples and the difference in the results between internal and induced stresses were compared. An investigation to verify if thermal healing methods can relieve the concentrations of stress within the material was also performed. The general process was made by inserting the sample into the polariscope, illuminating it with a white light source, capturing an image, saving the image in JPEG file format, converting the JPEG file into text format using a software, and finally analysing the numbers extracted from the digital images. The text illustrates that by extracting data from pictures, it is possible to analyse the stresses by observing the average light intensity in the pixels. The load and thermal healing analysis showed that the change in intensity is indeed depending on the magnitude of stress. Thermal healing also showed to be effective when relieving internal stress. It was also possible to observe the location where the stress is acting.

Keywords:	photoelasticity, stress concentration, PET, injection moulding, light intensity, digital images, thermal stress relaxation, polarized light
Number of pages:	73
Language:	English
Date of acceptance:	20.03.2018

Table of Contents

FIGURES

TABLES

ABBREVIATIONS

AVG	Average
IMM	Injection Moulding Machine
IMP	Injection Moulding Process
IR	near-, mid-, and far-infrared
JEPG	Joint Photographic Experts Group
PET	Polyethylene terephthalate
Pixel	Picture Element
PPL	Plane-Polarized Light
RGB	Red, Green, Blue
RP	Reflection Photoelasticity
TP	Transmission Photoelasticity
USB	Universal Serial Bus

Symbols

Variables	Description	Units [SI]
A	Cross-sectional area	$[m^2]$
C	Speed of light	$[m/s]$
F	Force	$[N]$
g	Gravitational acceleration	$[m/s^2]$
I	Intensity of light	$[W/m^2]$
K	Strain-optical coefficient	$-$
m	Mass	$[kg]$
N	Fringe order	$-$
N	Number of molecules per unit volume	$-$
n	Refractive index	$-$
P	Photoelastic coefficient	$-$
P	Internal resultant force	$[N]$
T	Temperature	[°C]
V	Speed of light in transparent bodies	$[m/s]$
V	Internal resultant shear stress	$[N]$
α	Polarizability	$[C \cdot m^2/V^{-1}]$
δ	Relative retardation	$[nm]$
ΔB_{ij}	Change in indicatrix under stress or strain	$-$
ΔI	Change in maximum intensity (RGB max)	$-$
Δ_s	Length of a line in an undeformed body	$[mm]$
Δ'_s	Length of a line after deformation	$[mm]$
ϵ	Strain	$-$
ϵ_{avg}	Average normal strain	$-$
λ	Wavelength	$[nm]$
ρ	Density	$[kg/m^3]$
σ_{avg}	Average normal stress	$[Pa]$
τ_{avg}	Average shear stress	$[Pa]$

FOREWORD

A very special thanks to my thesis advisor Mr. Rene Herrmann for all guidence and time invested throughout this research. Furthermore, I wish to express my appreciation to Arcada's Lectures, in special Mr. Mathew Vihtonen for all the valuable lessons and feedbacks that were essencial when writing this work. I would like also to thank Mr. Stewart Makkonen and Mr Erland Nyroth for all advice and direction given during my studies.

I also wish to thank my family and friends. In special my good friend Liuba Nikiforova for all the help and support. Lastly, a sincere thanks to my parents and husband Lauri Kotila for all the patience and words of encouragement.

Helsinki, March 2018

Gabriela dos Santos Kotila

1 INTRODUCTION

When developing a product there are important points to be considered before the design is created. An example is the choice of the best material to be used. There are several methods to determine different properties within a material. Having a good knowledge of the materials limitations is important to prevent failure of the product. Most methods of stress analysis investigate how a material will react under a force. These methods investigate the amount of stress which will cause the material to fail. With photoelasticity it is possible to investigate the stress on the surface and inside the material.

1.1 Background

Photoelasticity is an experimental stress and strain analysis technique based on an optical mechanic property referred as birefringence. [1] This property is possessed by many transparent materials such as crystals, glasses and some polymers. This stress-analysis technique is convenient when investing internal stress in products with complex shapes. The results obtained allow us to modify the part by relieving internal stress or removing materials from areas with low stress.

To perform photoelastic stress analysis a source of light is needed. Light is electromagnetic radiation that when propagates its waves go in all different directions. A polariscope is an instrument used when performing photoelastic analysis. When polarised light passes through a stressed transparent model, interference patterns or fringes are formed. [2]

The specimens used for this research were injection moulded. When injection moulding a product, multiple defects can happen. Some of these defects will cause concentrations of stress throughout the sample. One example of a defect is called thermal contraction of the product (shrinkage). If shrinkage of the plastic cannot be compensated in certain areas,

sink marks will occur during the cooling process causing stress concentrations in the product. [3]

One way to remove the internal stress in materials, is through stress relief. Stress relief can be done in many different ways such as thermal relaxation. In this method the part is heated uniformly in a constant temperature during a period of time. With thermal relaxation it is possible to obtain material yield strength reduction, stress redistribution, and elastic relaxation. [4]

1.2 Methodology

An experiment using PET samples was performed by a student also at Arcada University, however due to small stress concentrations on her samples it was not possible to observe a clear fringe pattern. [5] An experiment in composites using photoelasticity to analyse thermoplastic-thermoset interface (PET/Epoxy), revealed shear stress distribution through isochromatic fringe patterns. [6] Photoelastic coating technique method, also showed good results when used to analyse wooden beams reinforced with carbon fibre reinforced polymers. [7] All the research performed above studied the stresses in the samples by observing and counting the fringe patterns. In this work a different approach is used.

When performing a photoelastic stress analysis, digital images are captured from the samples. A digital picture is a collection of numbers. These numbers can be stored, modified, transmitted and converted into something that it is possible to see. Every scene captured in a digital image is a pattern of light and dark regions. These regions are divided into very little squares called a “pixel”. Every digital picture has numbers which describe the image. These numbers represent the average brightness (intensity) in each pixel, such as that the darkest part of the image is zero, and the lightest is 255. [8] In this research this range value from 0 to 255 is used to investigate the intensity of light in PET samples

due to stresses influence. Values close to 0 indicate small amount of stress while values close to 255 represent higher stresses.

1.3 Objectives

The research conducted in this paper is a qualitative research. Qualitative research seeks answers to a question, systematically uses a predefined set of procedures to answer the question, collects evidence, produces discoveries that were not determined in advance and produces findings that are applicable beyond the immediate boundaries of the study. Qualitative research is used to interpret and to better understand the complex reality of a given situation and the implications of quantitative data. [9] It is aimed to investigate throughout this paper the internal stresses in injection moulded PET samples. The main goals are

- Use photoelasticy to study the stress concentration caused during injection moulding process, and possible reasons which created the stress.
- Try to relieve the stress concentration using methods of stress relaxation such as thermal relief.
- Apply several loads in the samples and then analyse the difference in light intensity due to induced stresses.
- Extract data from the digital images and analyse the light intensity average in the pixel count caused by stresses in the sample.

This paper is divided into six chapters. The first chapter explains the importance of this research, the utilized methods and its main objectives. The second chapter presents a literature review about major topics needed to understand the research performed in this work. Chapter three describes how the experiments were performed and how the data was collected. In the fourth chapter the results obtained are presented. The fifth chapter discusses the results from the experiments. The sixth chapter concludes the findings of the research and presents alternative methods of analysis.

2 LITERATURE REVIEW

2.1 Mechanics of Materials

Mechanics of materials is the field which studies the effects of stress and strain in a solid body. These effects are a result of an external loading. While stress is associated with the strength of the material, strain is a measure of the deformation of the body. [10] Since Photoelasticity is a stress/strain analysis, it is vital to understand stress and strain definition in a body.

2.1.1 Stress

As described previously, stress is associated with the strength of the material. Let us consider figure 1. A load *P* is applied to the bar (c). The load acts through the centroid of its cross-sectional area. This will make the bar deform uniformly throughout the central region of its length. When separating the bar into two parts (d), equilibrium requires the resultant force at the section to be *P*. Due to the uniform deformation (material is homogeneous and isotropic) of the material, it is necessary that the cross section is subjected to a constant normal stress distribution.

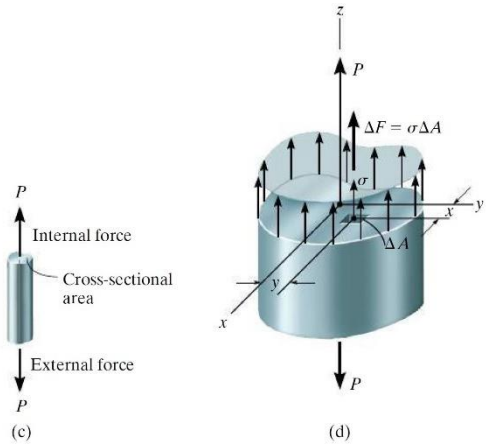

Figure 1: *Applied force on a bar and stress distribution on a sectioned area. [10]*

As a result, each small area ΔA on the cross section is subjected to a force $\Delta F = \sigma\, \Delta A$. The sum of these forces acting over the entire cross-sectional area must be equivalent to the internal resultant force **P** at the section. If $\Delta A \rightarrow dA$ and $\Delta F \rightarrow dF$, then recognizing σ as a constant it is obtained: [10]

$+\uparrow F_{rz} = \sum F_z;$ $\qquad \int dF = \int_A \sigma\, dA$

$$P = \sigma A$$

$$\sigma_{avg} = \frac{P}{A} \qquad (1)$$

Where,

σ_{avg} = average normal stress at any point on the cross-sectional area (Pa)
P = internal resultant force, which acts through the centroid of the cross-sectional area (N)
A = cross-sectional area of the bar where σ is determined (m^2)

Another category of stress is the average shear stress. Shear stress is the stress component that acts in the plane of the sectional area (figure 2) and it can be determined as: [10]

$$\tau_{avg} = \frac{V}{A} \qquad (2)$$

Where,

τ_{avg} = average shear stress at the section, which is assumed to be the same at each point located on the section (Pa)
V = internal resultant shear force on the section determined from the equations of equilibrium (N)
A = area at the section (m^2)

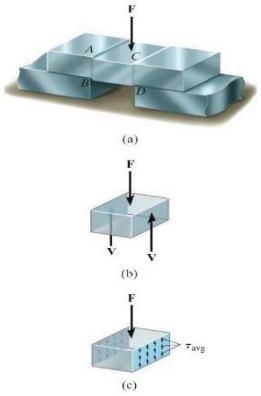

Figure 2: *Normal shear stress. [10]*

2.1.2 Strain

As mentioned previously, strain is a measurement of the deformation of the body. The normal average strain is defined as: [10]

$$\epsilon_{avg} = \frac{\Delta_s' - \Delta_s}{\Delta_s} \quad (3)$$

Where Δ_s (mm) represents the length of a line in an undeformed body and Δ_s' (mm) represents the length of the same line after deformation of the same body.

2.2 Injection Moulding Process

Injection Moulding is a polymer processing method used to create products in a certain desired shape. The plastic is poured into a hopper, then melted in a screw located inside the barrel. This screw rotates while melting the plastic. Later, the plastic is injected into a mould where it is moulded into the final product. An example of an injection moulding machine (IMM) and injection moulding process (IMP) can be seen from figure 3.

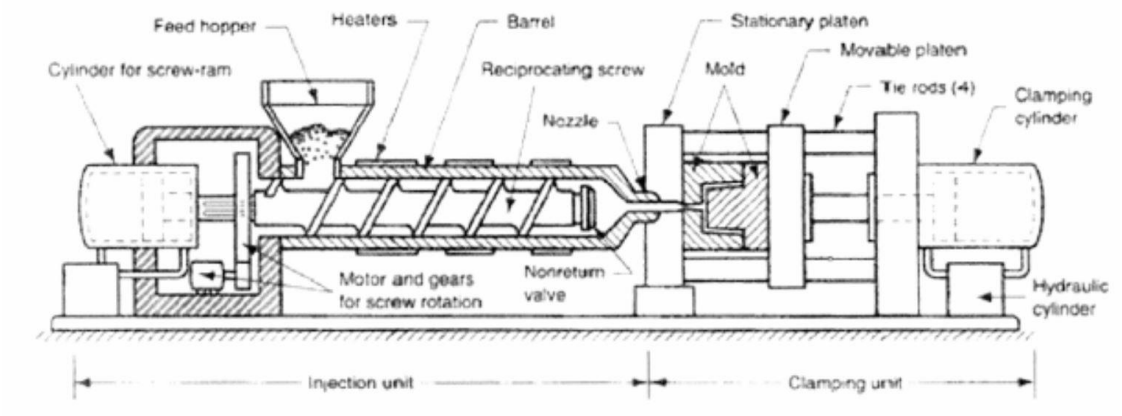

Figure 3: *Injection moulding process example. [11]*

2.2.1 Part Defects

One of the causes for stress concentrations in injection moulded parts is due to poor choice of settings in the parameters of the IMM. It is normal that the amount of stress concentration will probably be localized in the areas with drastic shape change, or where the material is poorly distributed.

Sink marks is one of the reasons for internal stress. Typically, sink marks occur during the cooling process. The cause for this, is because thermal contraction happens when the part is cooling. This is termed as shrinkage. When the product suffers shrinkage, sometimes the plastic cannot be compensated in certain areas. This could be related to slow solidification, not enough time for effective holding pressure, or not enough holding pressure transfer because the flow resistances in the mould are too high. [3] Figure 4 shows an example of sink marks in a product.

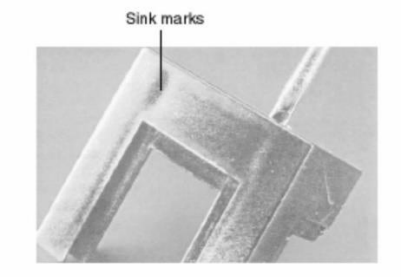

Figure 4: *Sink marks due to wall thickness variations. [3]*

To prevent sink marks, a change in the settings of the machine is necessary.

2.3 Polyethylene Terephthalate

2.3.1 Material Description

Poly(ethylene terephthalate), PET or PETE is an oil based material and it is a widely used semicrystalline polymer from the polyester family. Whinfield and Dickson, (England) were the ones who formed for the first time the polyester. They did this by employing an ester interchange reaction between ethylene glycol and methyl ester of terephthalic acid. [12] Figure 5 shows this reaction.

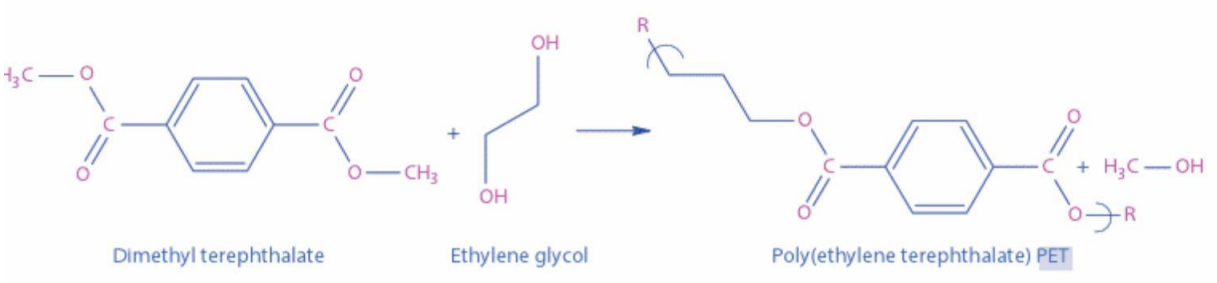

Figure 5: *PET reaction. [12]*

While PET is normally made from the reaction above, it can also be made from the ring opening reaction with ethylene glycol as shown below.

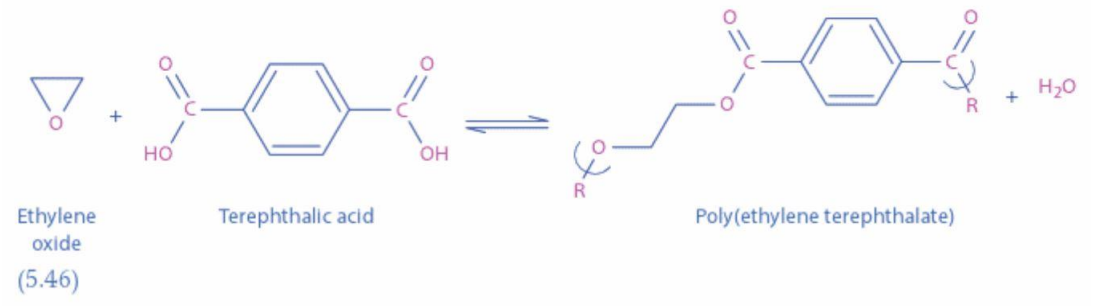

Figure 6: *Ring opening reaction with ethylene glycol. [12]*

The microscopic properties of PET such as, thermal, permeation and the most important property for this work the optical property depends on its specific internal morphologies and microstructure arrangement. [13] PET may appear opaque, white or transparent depending on its crystalline and amorphous structure. [14]

2.3.2 Absorption by Visible and Ultraviolet Light

The absorption of photons is associated to their interaction with the outer shell electrons. The photons energies range from 1.6 eV ($\lambda = 800\ nm$) to about 6.2 eV ($\lambda = 200\ nm$), where eV is the electronvolt and λ is the wave length. The time scale for absorption is about $10^{-15}\ s$. There are two prerequisites for the absorption of a photon of energy hν by a polymer. The first requisite is that the molecule must contain a chromophoric group with excitable energy states corresponding to the photon energy. The second is that the transition between the two energy group states is required to cause a change in the charge distribution within the molecule e. g., a change in the dipole moment. [15]

2.3.3 Absorption by Infrared Radiation

The infrared portion of the electromagnetic spectrum is normally divided into the near-, mid-, and far-infrared (IR) regions. In the case of small molecules, the IR photon energies correlate to rotational motions. For large molecules it correlates to collective intramolecular and intermolecular vibrational modes (far-IR), fundamental vibrations (mid-IR), and to overtone and combination vibrations (near-IR). The molecules rotate, and the atoms of the molecules vibrate at frequencies correlating to the discrete energy level. The shape of molecular potential energy surfaces, the mass of the atoms, and the association vibronic coupling determine the discrete level. There are also two conditions necessary for the absorption of emission of IR of frequency ν. In the first condition, the photon energy hν must correspond to the difference of discrete energy levels. The second condition is the same presented in the absorption by visible and ultraviolet light. If the

molecules in the unit cell of crystalline polymers are placed close enough together, the interaction of polymers chains can result in a detectable effect. [15]

2.4 Photoelasticity

2.4.1 Definition

Photoelasticity is an experimental stress analysis. This technique uses amorphous materials (such as crystals, glasses and polymers). Mediums containing this property are isotropic when unstressed and when stressed they become anisotropic. [16] Isotropic materials, contain the same physical and mechanical properties throughout its volume in all directions. [10]. In anisotropic materials the properties change with the direction. This optical effect is referred to as temporary optical birefringence and it was observed the first time by Sir David Brewster (1816). [16]

Photoelastic stress analysis has become a technique of outstanding importance to engineers over the years. Engineers have been able to use photoelasticity as a method of stress/strain analysis to analyse bodies with complicated shapes.

The fringe patterns formed when polarized light passes through a stressed transparent model, provide immediate qualitative information. These informations give us general distribution of stress, positions of stress concentrations and areas of low stress. Once these results are obtained, the designs can be modified. After a photoelastic stress analysis we can immediately notice if stress concentration in the areas of the body needs to be reduced or dispersed, or if excess materials need to be removed from areas of low stress. Photoelastic analysis provides an effective method of failure investigation, reduction in weight and material cost, and often produces valuable information leading to succesful re-design. [17] Figure 7 shows the photoelastic effect.

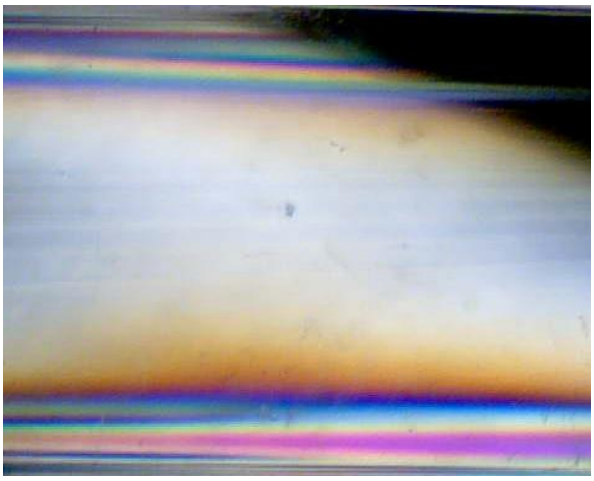

Figure 7: *Photoelastic effect. Arcada, 2018*

2.4.2 Photoelastic Properties of Materials.

Photoelasticity has already been defined as a stress/strain analysis technique which utilizes the photoelastic effect. The photoelastic effect was described as a property of some transparent materials. In this section will be shown the property in a molecular level. On the following will be explained why certain materials have this property.

When a material possesses a sizable photoelastic coefficient (*p*), this material is required to enhance the interaction between mechanical strain ϵ and refractive index *n*. The change in indicatrix is defined as: [18]

$$\Delta\left(\frac{1}{n^2}\right) = p\epsilon \qquad (4)$$

The optical indicatrix is a single-valued surface which specifies the relationships between refractive indices, wave normals, polarization directions, and energy flow directions (= ray directions). [18]

Since strain and refractive index are dimensionless, photoelastic coefficients also are. To clarify the effects of stress on refractive index, it will be considered the effect of

hydrostatic pressure on a crystal cube. The following equation is the Lorenz-Lorentz equation and it is valid for many cubic materials [18].

$$\frac{n^2-1}{n^2+1} = KN\alpha \qquad (5)$$

Where,

K is a proportionality constant
N is the number of molecules per unit volume
α is the polarizability per molecule ($C \cdot m^2/V^{-1}$)

Differentiating with respect to density ρ (kg/m^3) , gives,

$$\frac{dn}{d\rho} = \frac{(n^2-1)(n^2+2)}{6n\rho}\left(1 + \frac{\rho}{\alpha}\frac{d\alpha}{d\rho}\right)$$

This leads to an estimated photoelastic coefficient *p* [18]

$$p = \frac{(n^2-1)(n^2+2)}{3n^4}\left(1 + \frac{\rho}{\alpha}\frac{d\alpha}{d\rho}\right) \qquad (6)$$

As the pressure increases the atoms will pack together, which will cause an increase in refractive index. Therefore, it can be concluded that the refractive index is a function of pressure through density and polarizability. [18]

The photoelastic effect concerns the changes in optical indicatrix with mechanical stress or strain. For an arbitrary coordinate system (Z_1, Z_2, Z_3) the indicatrix takes the form $B_{ij}Z_iZ_j = 1$. The changes in the indicatrix under stress σ_{ki} or strain ϵ_{ki} are represented through the linear relation [18]:

$$\Delta B_{ij} = \pi_{ijki}\sigma_{ki} \qquad (7)$$

Or

$$\Delta B_{ij} = p_{ijki}\epsilon_{ki} \qquad (8)$$

The coefficients π_{ijki} and p_{ijki} are fourth polar rank tensors. Since stress and strain are related to one another through the elastic constants, π and p coefficients also are. Both the indicatrix and the strain tensor are symmetric, so that $B_{ij} = B_{ji}, \epsilon_{kl} = x_{lk}$, and $p_{ijkl} = p_{jikl} = p_{ijlk} = p_{jilk}$. This means that 36 coefficients in a 6 X 6 matrix are sufficient to describe the linear photoelastic effect: [18]

$$\begin{pmatrix} \Delta B_1 \\ \Delta B_2 \\ \Delta B_3 \\ \Delta B_4 \\ \Delta B_5 \\ \Delta B_6 \end{pmatrix} = \begin{pmatrix} p_{11} & p_{12} & p_{13} & P_{14} & P_{15} & P_{16} \\ p_{21} & p_{22} & p_{23} & P_{24} & P_{25} & P_{26} \\ p_{31} & p_{32} & p_{33} & P_{34} & P_{35} & P_{36} \\ P_{41} & P_{42} & P_{43} & p_{44} & P_{45} & P_{46} \\ P_{51} & P_{52} & P_{53} & P_{54} & p_{55} & P_{56} \\ P_{61} & P_{62} & P_{63} & P_{64} & P_{65} & p_{66} \end{pmatrix} \begin{pmatrix} \epsilon_1 \\ \epsilon_2 \\ \epsilon_3 \\ \epsilon_4 \\ \epsilon_5 \\ \epsilon_6 \end{pmatrix} \qquad (9)$$

2.4.3 Two and Three-dimensional Photoelasticity

Two-dimensional photoelasticity means that the thickness of the model is uniform and also small when compared with the other dimensions in the plane. [19] Three-dimensional photoelasticity is related to parts where the stress varies not only as a function of the shape in one plane, but also throughout the thickness. [17] From here on it will be considered the stress analysis made in a model with uniform thickness. Therefore, the importance will be in two-dimensional models.

2.5 Transmission Photoelasticity

For many years conventional or transmission photoelasticity (TP) has been a powerful tool in the hands of engineers to make stress analysis. Hearn in his book gives a general idea of what can be done with TP technique.

"*A major feature of the technique is that it allows one to effectively "look into" the component and pin-point flaws or weaknesses in design which are otherwise difficult or impossible to detect. Stress concentrations are immediately visible, stress values around the edge or boundary of the model are easily obtained and, with a little more effort, the separate principal stresses within the model can also be determined."* [17] (p. 182)

Here will be discussed the methods of both (TP) and reflection photoelasticity (RP). The TP method is presented before because RP is only an extension of the TP method used to analyse opaque parts. Once it is clear how TP technique works, it will be only necessary to light up the differences between one and the other.

2.5.1 Light

Before explaining what polarized light is, it will be explained first what light is. A general definition given by encyclopaedia Britannica defines light as "*electromagnetic radiation that can be detected by the human eye.*" [20]

To perform a stress analysis test using photoelasticity, it is fundamental to have a light source. There are two main sources of light and they are incandescence and luminescence. Incandescence light is defined as the emission of light from "hot" matter ($T \geq 800$ K), while luminescence light is the emission of light when excited electrons fall to lower energy levels. [21] Frequency in physics is the number of waves that pass a fixed point in unit time, also, the number of cycles or vibrations undergone during one unit of time by a body in periodic motion. [22] The frequency of light is related to its colour. There are two main groups: monochromatic and polychromatic. [21]

Monochromatic light is described by only one frequency. One example of monochromatic light is laser light.

Polychromatic light is described by many different frequencies and one example of polychromatic light is white light.

2.5.2 Refraction and Retardation

Light propagates in a vacuum or in air at speed *C* of $3.00 \times 10^8\ m/s$. When it comes to transparent bodies, the speed (defined as *V* for transparent bodies) is lower. [2] In physics, refraction is defined as the change in direction of a wave passing from on medium to another caused by its change in speed. [23] Snell's law states that "*the ratio of sines of the angles of incidence and refraction is equivalent to the ratio of velocities in two media, or equivalent to the opposite ratio of the indices of refraction*." [24] (p.141) Figure 8 shows the refractive index when light passes from one medium to another.

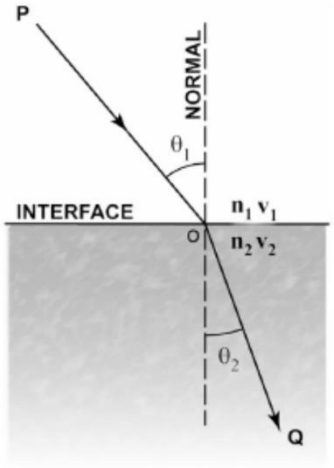

Figure 8: *Refractive index when passing from one medium to another. [24]*

The figure above shows the incident wave front represented by a ray that is by the normal to the plane utilizing the geometrical optics approximation. The Snell's law takes then the form: [24]

$$n = \frac{sin\,\theta_1}{sin\,\theta_2} \qquad (10)$$

Considering what was said previously, the refractive index equation can be rewritten using the velocity of light c of a given wavelength in empty space divided by its velocity *v* in a substance. [25]

$$n = \frac{C}{V} \qquad (11)$$

where C is the speed of light (*m/s*) and V is the speed of light coming through a transparent medium (*m/s*). A transparent plastic of thickness *t*, has the ability to split an incident plane-polarised ray into two component rays, which are called double refraction. This property is only exhibited when the materials are under stress and for this reason it is termed "temporary birefringence*"*. [17] Consider a specimen that is being analysed, let us take X and Y as reference directions of the principal strains at the point under consideration where the light vector splits. If the strain intensity along X and Y is ε_x and ε_y, and the speed of the light vibrating in these directions is V_x and V_y, respectively the ratio *t/V* will be the time necessary to cross the plate for each of them. Considering this statement, the relative retardation between these two beams can be defined as: [2]

$$\delta = C\left(\frac{t}{V_x} - \frac{t}{V_y}\right) = t(n_x - n_y) \qquad (12)$$

According with Brewster's law "*The relative change in index of refraction is proportional to the difference of principal strains*" [2] (p. 2)

$$(n_x - n_y) = K(\varepsilon_x - \varepsilon_y) \qquad (13)$$

K characterizes a physical property of the material and is defined as a constant termed "strain-optical coefficient*"*. K is a dimensionless constant that it is usually established by calibration and may be considered similar to "gage factor" of resistance strain gages. When combining the expressions shown above, the relative retardation for TP is obtained. [2]

$$\delta = tK(\varepsilon_x - \varepsilon_x) \qquad (14)$$

Once relative retardation occurs, the two waves are no longer in phase when emerging from the plastic. The resulting light intensity will be a function of retardation δ and the angle between the analyser and the direction of principal strains (β – α). [2]

If the original light source is monochromatic, the fringe pattern appears as a series of distinct black lines on a uniform green or yellow background. These black lines are the points where the two rays are exactly 180° out of phase and therefore cancelled. In the other hand, if white light is used each composite wavelength of the light is cancelled in turn and a multicoloured pattern of fringes called isochromatic is obtained. [17]

For accurate quantitative measurements it is preferable the use of Monochromatic sources. This is because of the high number of fringes (stress concentration) that can be discerned clearly. With a white light source, however, the isochromatic becomes very pale at high stress regions and clear fringe boundaries are no longer obtained. For this reason, white light sources are normally reserved for general qualitative assessment of models. [17]

2.6 Polariscopes

In experimental mechanics the main optical arrangements are called polariscopes. Polariscopes can be defined as interferometers that in the final superposition of the light vectors project the vector into a common direction. [24]

2.6.1 Plane Polarized Light

When light propagates, its electromagnetic waves will propagate in all directions. Now it is introduced the meaning of plane-polarized light and its use in the equipment termed polariscope. Let us consider an ordinary light bulb illuminating a polarizer or sheet. When the light passes through it, the polarizer will act like a series of vertical slots. When the light emerges from the polariser, it will vibrate in one plane. This will be the plane of the slots. The light is then said to be plane polarized. [17]

When the plane polarised light (PPL) is directed onto an unstressed photoelastic specimen, it will pass unaltered and may be completely extinguished by a second

polarising sheet. This second sheet is termed analyser, and its axis is perpendicular to that of the polarizer. This is considered the simplest form of polariscope arrangement which can be used for photoelastic stress analysis. This form of polariscope arrangement is termed: “crossed” set-up [17] which is shown in the next figure:

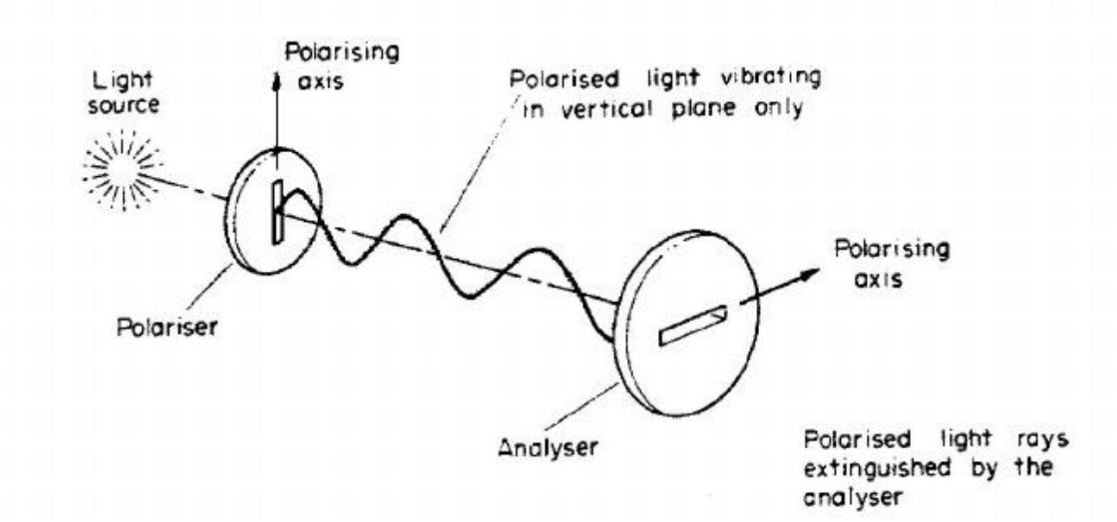

Figure 9: *"Crossed" set-up. plane polarised. [17]*

There is an alternative polariscope arrangement called “parallel” set-up. In this case the PPL will then pass through both the model and the analyser unaltered and maximum illumination will be achieved. [17] An example of a parallel set up is shown below:

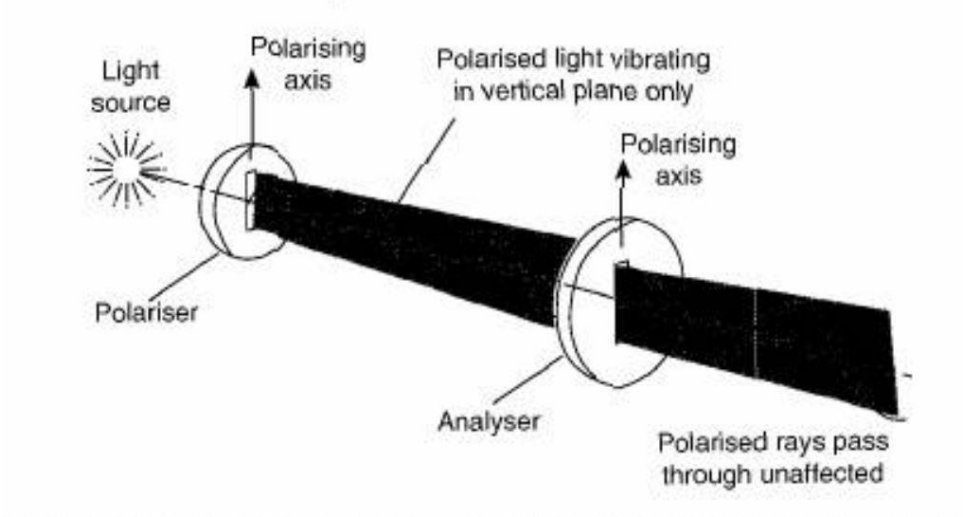

Figure 10: *"Parallel" set-up. plane polarised. [17]*

Entering a medium (for example a plastic with thickness *t*), the wave is divided into two waves with their vector x and y vibrating in perpendicular directions orthogonal to the normal of the wave. The analyser transmits only the components along its axis. [24] A plane polariscope arrangement example is shown in figure 11.

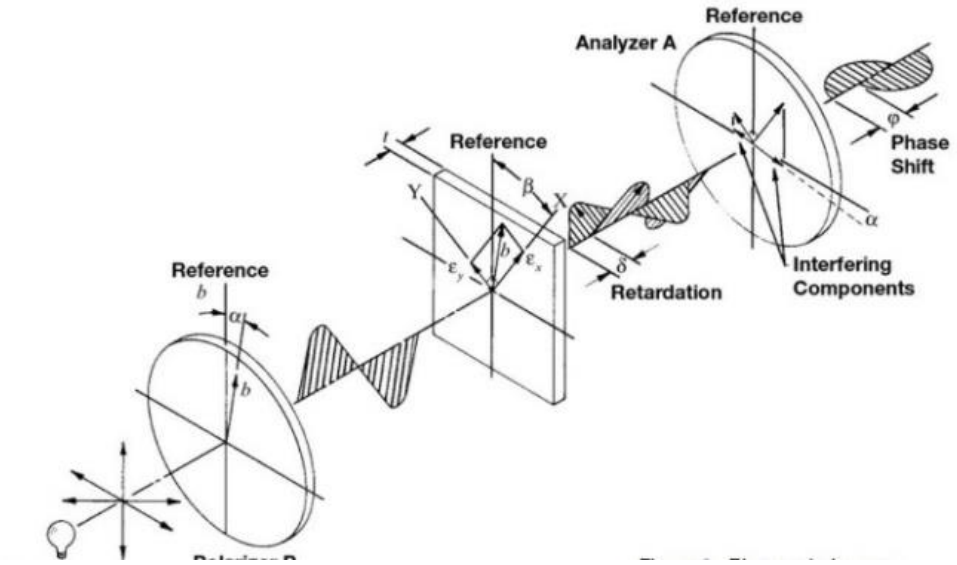

Figure 11: *Plane polariscope. [2]*

The intensity of light emerging from a plane polariscope is: [2]

$$I = b^2 \sin^2 2(\beta - \alpha) \sin^2 \frac{\pi\delta}{\lambda} \qquad (15)$$

Where,

δ is the relative retardation (*nm*)
(β – α) is the difference between the angle between the analyzer and direction of principal strains
λ is the wavelength (*nm*)

A plane polariscope setup is used to measure the principal stress/strain directions. [2]

2.6.2 Circularly Polarised Light.

When analysing a sample using plane polarized light, the fringes or isochromatic that will generate in the part will be partially obscured by a set of lines known as isoclinic. If the source of light used is a white light source, these isoclinics are easily identified because of the coloured isochromatic of a white light. With a monochromatic source however, confusion can arise between the black fringes and the black isoclinics. [17] Therefore, it is of greater interest to use a different optical system which will eliminate the isoclinics but at the same time will retain the basic fringe pattern. They are removed optically by inserting quarter-wave plates (a member that behaves exactly like a photoelastic model having uniform birefringence of $N = 1/4$) with their axis at 45° to those of the polarizer and analyser. This eliminates all unidirectional properties of the light by converting it into circularly polarized. [19] A circular polariscope arrangement can be seen below.

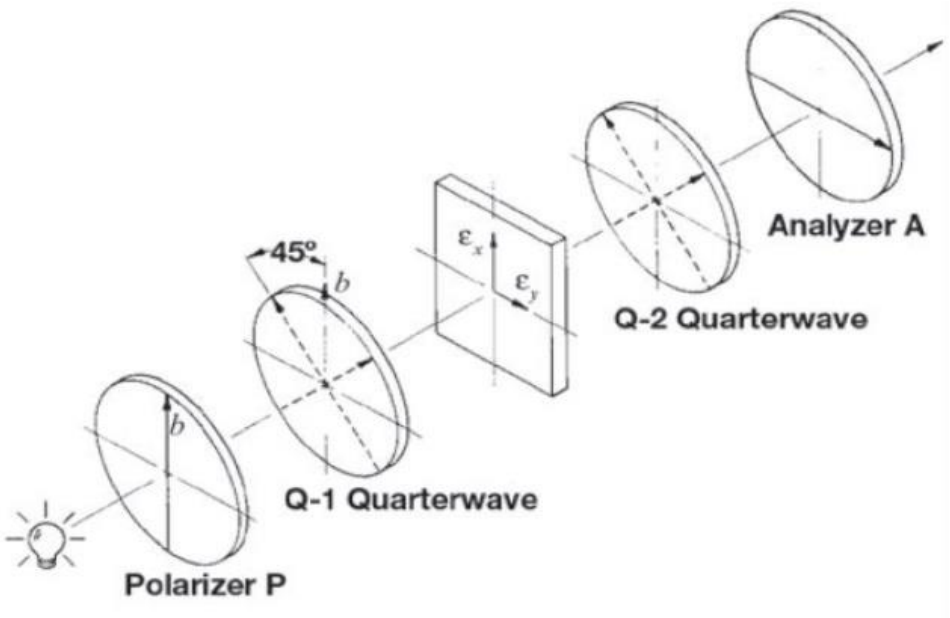

Figure 12: *Circular polariscope. [2]*

The result is then that the image observed is not anymore influenced by the direction of principal strains. The intensity of emerging light thus becomes: [2]

$$I = b^2 \sin^2(\pi N + \beta) \qquad (16)$$

where β is the angle of analyser rotation from the normal (crossed) position. The light becomes 0 (I = 0), when $(\beta + \pi N) = 0°, 180°, 360°, etc.$ [19]

2.7 Reflective Coating Technique

A reflection polariscope used in PhotoStress analysis, is a tool to observe and measure the surface strains on the photoelastically coated test part. [2] As described before, RP is an extension of the TP. RP technique helps us to analyse samples of materials that do not have photoelastic property.

This adaptation utilizes a thin sheet of a photoelastic material which is bonded onto the surface of a metal component. The material is bonded using a special adhesive containing aluminium pigment which produces a reflective layer. When using a reflection polariscope, polarized light is directed onto the photoelastic coating and viewed through an analyser after reflection of the materials surface. [17]

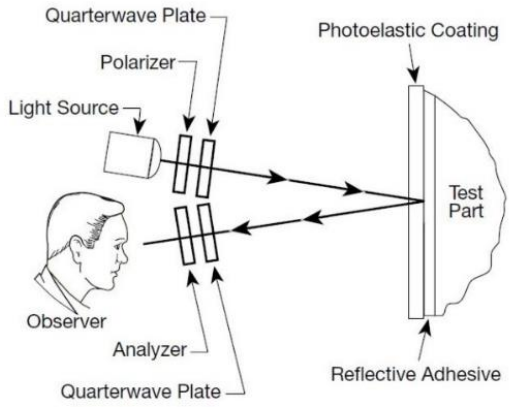

Figure 13: *Schematic representation of reflection polariscope. [2]*

The relative retardation of a reflective polariscope is: [2]

$$\delta = 2tK(\epsilon_x - \epsilon_y) \qquad (17)$$

The technique allows the evaluation of strains under loading conditions. A fringe pattern is observed which relates to the strain in the metal component. Unlike the transmission technique RP gives no information about the stresses within the material. [17]

The selection of PhotoStress coatings and their proper application to the test part are most essential to the success of the analysis. Coating materials are available in both flat-sheet and liquid form for application to metals, concrete, plastics, rubber and most other materials. [2]

2.8 Digital Images

To perform Photoelastic analysis it is necessary to capture pictures from the samples. In this work, the values representing the dark and light regions of an image is used to analyse the stress in the samples. This chapter will describe the relations between the pixels in an image and light intensity.

2.8.1 Pixel and Light Intensity Relation

Inside a digital picture lies a collection of numbers. These numbers can be stored, modified, transmitted and converted into something which is possible to see. A digital image creation can be described in three steps. The first step would be the selection of an area or scene to be captured. Every scene is a pattern of light and dark regions. The process ignores the objects in the pictures and only deals with dark and light. Once the image is captured the second step would be to divide the digital image into little squares. Each square is called a “pixel”, what is an abbreviation for “picture element”. The third step creates the numbers which describe the image. These numbers represent the average intensity in each pixel, such as that the darkest part of the image is zero, and the lightest is 255. There are many small variations on this “digitalization” process and often the range of 0 to 255 is used because each of these numbers can be stored in one byte of

memory. [8] In this work these numbers represent the light intensity, where at 0 there is no intensity and 255 represents maximum intensity.

The range of 0 to 255 is emphasised because this is the range used in the Joint Photographic Experts Group (JPEG) file format. This is the file format used to store the images used for the analyses discussed throughout this paper. JPEG file, represents a series of techniques aimed at reducing the redundancy present in the data, to allow more image to be recorded on a memory card. [26] The brightness value or digital count of two neighbouring pixels is very similar (if not the same) in magnitude. When this is the case, it is not needed to use all the data in an image to represent the information in the photograph. This type of redundancy made by the JPEG file, is called inter-pixel redundancy. [27]

The number of pixels in a JPEG file is represented by the file's dimension, e. g. an image with dimensions 640 *X* 480 contains 307200 pixels. It is possible to observe this relation from figure 14. The figure shows a pixel grid 10 by 10 rows and columns.

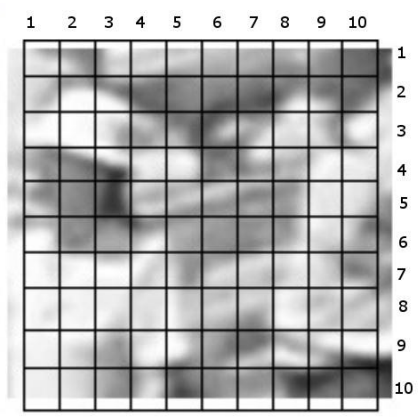

Figure 14: *10 X 10 Pixel grid. [8].*

In a digital image each pixel must contain values representing all the three primary colours RGB (Red, Green and Blue). These values describe accurately the final colour of the pixel. When an image is captured, each pixel on the imaging sensor records only the

value of one of those colours. For this reason, the other values must be calculated based on surrounding values. [26]

2.9 Residual Stress Relaxation Method

As mentioned previously, photoelasticity is a technique which gives us information about the general stress distribution, position of stress concentration and areas where there is low stress.

Based on the results from the photoelastic analysis it might be necessary to make design changes on the product in order to relief stress concentrations in certain areas. Here will be presented a technique called thermal relaxation used for stress relief.

2.9.1 Thermal Stress Relaxation

For thermal stress relaxation there is a technique called isothermal stress relief. This technique involves heating a part uniformly and holding it at a suitable temperature for a certain period of time. The tool used to do this is usually an air circulation furnace with good control over the specified thermal cycle. [4]

With thermal stress relaxation, it is possible to obtain the following stress relief results: [4]

- **Material yield strength reduction.** If the temperature is high enough it will cause a substantial material yield strength reduction. This happens because the plasticity mechanisms through rapid thermal activation will relieve the elastic strain.

- **Stress redistribution.** This is achieved by using lower temperatures. This is possible because at the regions of tensile and compressive stresses can contract or

expand slightly. Classical diffusional creep enables the counterbalancing of these regions.

- **Elastic stress relaxation.** This is obtained by precipitation and ageing effects.

Since all these processes are time dependent, it is really important to know the appropriate temperature and the time duration required to achieve the desired result. The determination of the temperature is often accomplished by experimenting. [4]

3 METHOD

3.1 Materials and Tools

The material chosen to be analysed is polyethylene terephthalate (PET or PETE). The reason for this choice is due to the transparency and optical properties of PET already described in previous chapters. The samples provided for the experiments were injection moulded by Arcada's lab engineer. There is no information on the parameters used in the IMM when the samples were processed. The samples are dumbbell shaped, with the following dimensions: thickness = 0.003 *m*, width = 0.019 *m* and length = 0.17 *m*. A sample is shown in figure 15.

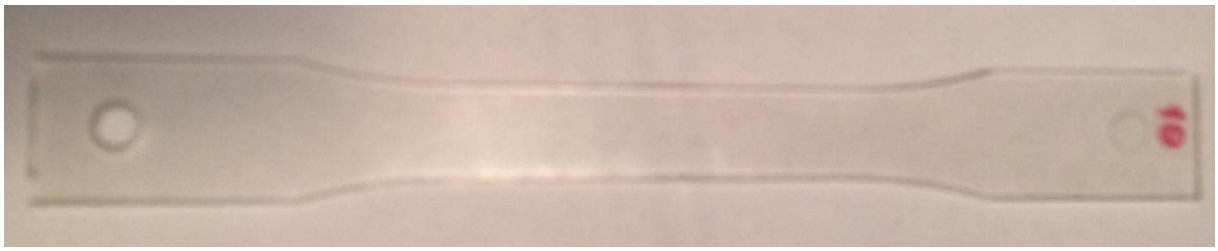

Figure 15: *PET sample used for photoelastic analysis. Arcada, 2018*

The instrument used is composed of a plane polariscope, a white light source, an USB camera, and a computer (figure 16). The general process was made by inserting the sample in the polariscope, illuminating it with the white light, capturing an image, saving the image in JPEG file format, converting the JPEG file into text format using a software, and finally analysing the numbers extracted from the digital image.

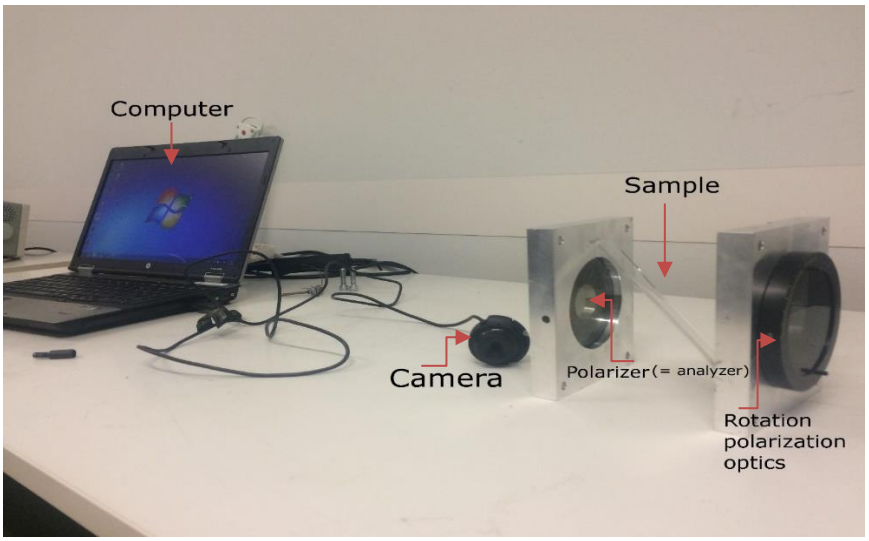

Figure 16: *Experiment set-up. Arcada, 2018*

3.1.1 Polariscope

The polariscope arrangement can be seen from figure 17.

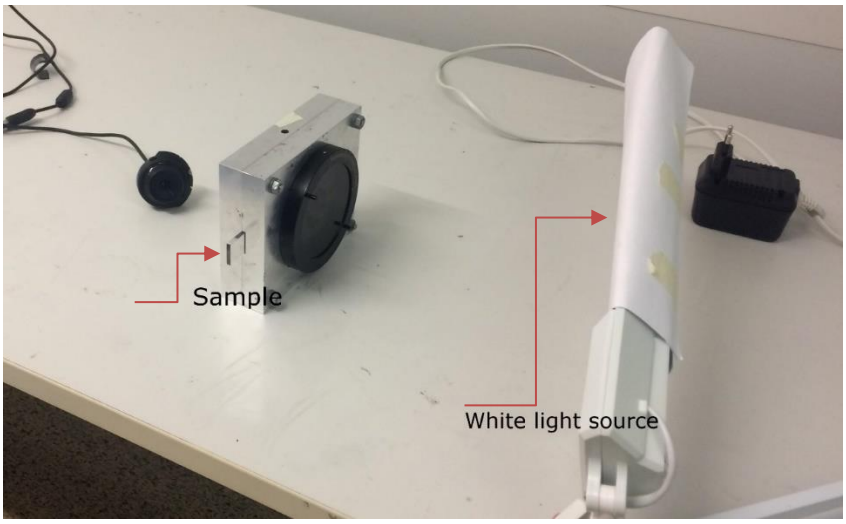

Figure 17: *Polariscope arrangement. Arcada, 2018*

First step was to insert the sample in the polariscope. To do this the polariscope was unscrewed and the sample was attached inside, then the instrument was screwed back together. The polariscope was then turned in a way where the sample would be in a vertical position. The side with the rotation polarization optics was facing the light source

and the camera was placed at the back of the polariscope with its USB cable attached to the computer. A paper was used to soften the light brightness and focus its direction (as shown in figure 17).

The polariscope used for our experiments did not have numbers marking the angles. In other words, it was not possible to know accurately the used angle since the tool did not contain any sort of angle indication. Therefore, in order to perform the experiments, the visual lines representing the angles were assigned a variable α. When rotating the polariser, a line would be taken as reference, and to this reference line would be assigned a value $\alpha + 0$. From the reference line, the counting would be made in an interval from 10 to 10 until 90 e. g., $\alpha + 0$, $\alpha + 10$, $\alpha + n$,…,$\alpha + 90$. The following figure shows an example on how the angles where marked.

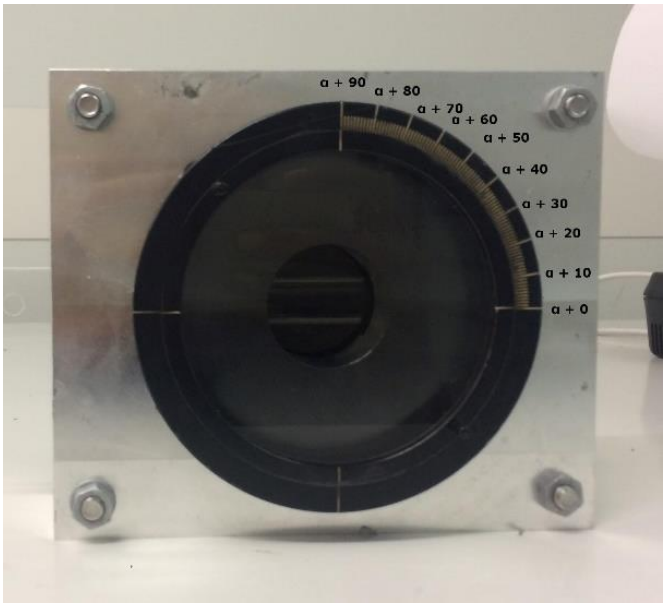

Figure 18: *Angle's assigned values. Arcada, 2018*

Once everything was adjusted in the correct place the room light would be switched off and the light source used for the experiment would be switched on. Then the angle in the polarizer would be rotated in a way where the least light intensity would come through. This was made with the intention of getting only enough intensity to see the internal stress

within the samples. Once the angle for each sample was adjusted, the same angle would be used for all the other experiments.

3.1.2 Images Capture

When the sample is illuminated inside the polariscope the observations of the internal stress is made through the computer. This is done by using the camera placed in the back of the polariscope and connected to the computer. In the settings it is possible to choose the images in colour or black and white. Once the light, the sample, and the angle have been adjusted in the desired way, the next step which is capturing the images can be made.

3.2 Experiments

3.2.1 Internal Stress Investigation

The process described above was made with ten different samples. The experiments were also performed with no samples inside the polariscope. For the later one, the polarizer was rotated from 10 to 10 degrees until 90 degrees. This was made to create a graph where the light intensity curve would not suffer interference due a medium. This graph was then used as reference to compare the changes in the light intensity curve due to stress in the load experiment. From the ten samples analysed, three were chosen to perform the load and thermal healing experiments. Samples 2, 7 and 8.

3.2.2 Induced Stress Using Different Loads

The load experiment was performed by making a 5-mm diameter hole in the samples where it was possible to insert a rope with a weight in its end. Figure 19 shows how the weights were attached to the sample.

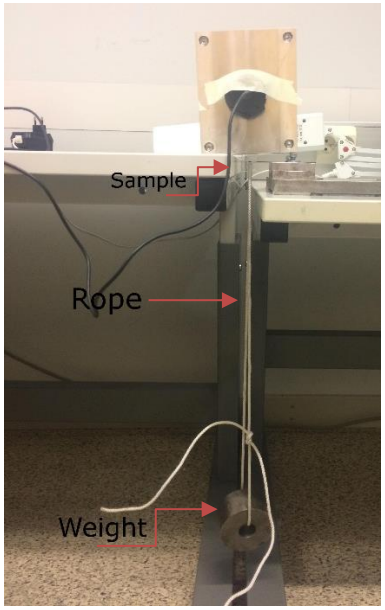

Figure 19: *Load experiment example. Arcada, 2018*

In total, eight loads and combination loads were used. The different used loads are shown below:

Table 1: *Loads used for photoelastic experiment. Arcada, 2018*

Load [kg]	Load [N]
0.366	3.59046
1.82	17.8542
2.546	24.97626
4	39.24
5.378	52.75818
6.832	67.02192
7.558	74.14398
9.012	88.40772

Where the loads in *N* where calculated from: [10]

$$F = mg \qquad (18)$$

A picture registering the change in stresses was then taken from each sample.

3.2.3 Thermal Healing Experiment

Thermal healing was performed in samples 2, 7, and 8. In the first attempt, the samples were kept in the oven at 50°C for 24 hours. Another attempt aiming to obtain a better result was made by increasing the temperature 30 degrees (80°C), and then keeping the samples again in the oven for 24 hours.

3.2.4 Data Extraction

In order to analyse the digital images, it was necessary to extract the numbers data from the JPEG files. To do this, a software was used. The following command was inserted in the conversion software to convert the files: "*convert (file name).jpg -define histogram:unique-colors=true -format %c histogram:info:- > (file name).txt"* (figure 20) The pictures were then converted from JPEG files to Text files.

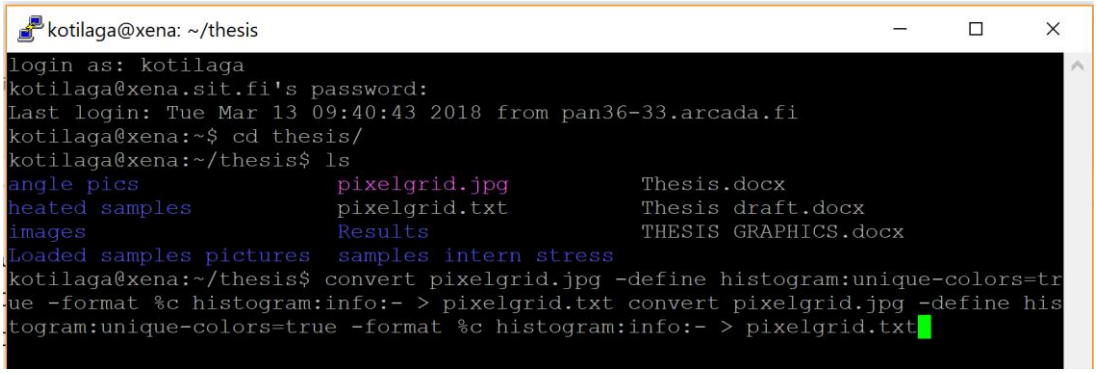

Figure 20: *jpg conversion to txt. Arcada, 2018*

The numbers in the text file were then inserted into Excel. After doing this it is possible to obtain the RGB and pixel count values, as shown in Figure 21.

pixel count	R	G	B
294451	0	0	0
4181	1	1	1
2673	2	2	2
1891	3	3	3
1221	4	4	4
753	5	5	5
436	6	6	6
304	7	7	7
171	8	8	8
111	9	9	9
91	10	10	10
78	11	11	11
98	12	12	12
89	13	13	13
80	14	14	14
65	15	15	15
47	16	16	16
56	17	17	17
61	18	18	18
63	19	19	19
47	20	20	20
50	21	21	21
37	22	22	22
51	23	23	23
23	24	24	24
20	25	25	25
8	26	26	26
12	27	27	27
14	28	28	28
6	29	29	29
4	30	30	30
5	31	31	31
2	32	32	32
1	34	34	34

Figure 21: *RGB values and pixel count from a random sample. Arcada, 2018*

The RGB max was then calculated using Excel's Max formula:

$$V = max(R, G, B) \qquad (19)$$

Once the RGB max is calculated a graph using these numbers can be created. The numbers on the y axis represent the digital count and the numbers in the x axis the RGB max values. The digital count is the number of pixels in a peak located in the graph's curve and the RGB max represents the intensity range in each pixel (the range from 0 to 255).

It is possible to see below an example of a graph made from a random black and white image:

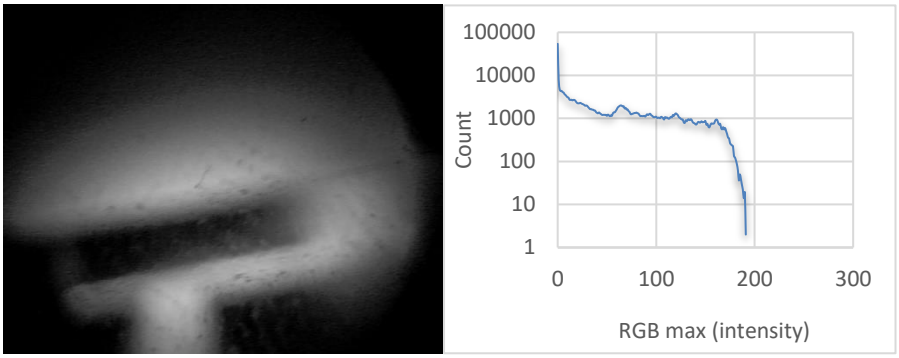

Figure 22a and 22b: *Black and white image intensity graph. Arcada, 2018*

A higher curve does not mean higher stress, instead it means a higher area of stress. The y axis represents the number of pixels in which the stress is acting. The amount of stress is represented in the x axis by the RGB max which is the average intensity. The higher the number of RGB max the higher the stress is. The following figure represents how a graph will look like with different stresses. Figure 23a, represents how a sample's graph would look like if no stress would be acting on it. Figure 23b shows a graph representing homogeneous stress. Figure 23c demonstrates how the curve could be like if there is stress distribution in the sample.

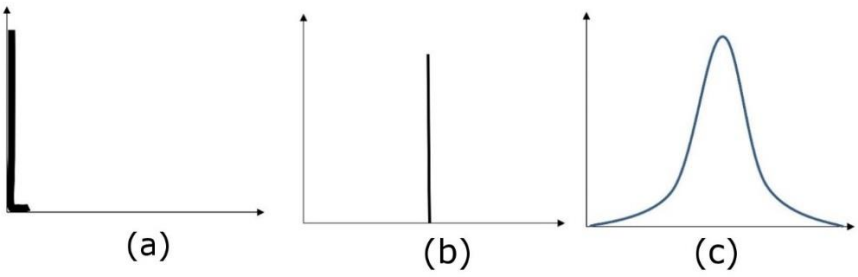

Figure 23a, 23b and 23c: *Representation of different possible stresses in a count-intensity graph. Arcada, 2018*

The data is then ready to be analysed.

4 RESULTS

4.1 Light Intensity Relation

As defined in chapter two in equation 15, the intensity of light emerging from a plane polariscope is

$$I = b^2 \sin^2 2(\beta - \alpha) \sin^2 \frac{\pi\delta}{\lambda}$$

As described previously, a new method is utilized to analyse the stress data obtained from the experiments. The light intensity is observed from the RGB max calculated from the picture's data, therefore, this equation is not utilized to analyse the experiment's results. Even though equation 15 is not used in this work, it is possible to observe its relationship with the graphs. A graph representing this equation will show a group of curve patterns caused by the $\sin^2$. If figure 24 is observed, it is possible to see these patterns forming as the intensity is increased. The graph from figure 24, is the graph obtained from the pictures of each angle from 0 to 90 without the interference of a medium. This was made with the aim of using the graph obtained from these pictures to compare with the graph created from the load experiment. The polarizer was rotated in steps of 10 to 10 beginning from α + 0 α + 10, α + n,…, to α + 90.

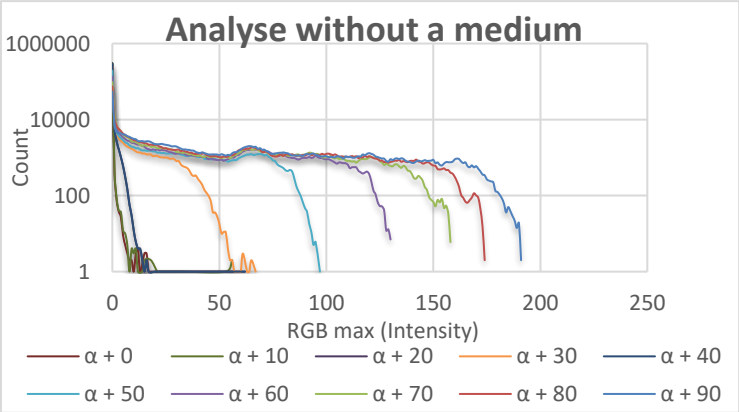

Figure 24: *Intensity curve represented in a graph. Arcada, 2018*

At 0° it is expected no light intensity coming through the polarizer and at 90° it is expected maximum intensity. From the graph it can be observed that light has its smallest intensity at α + 0 (where intensity is close to 0) and its highest intensity at α + 90 (where intensity is close to 190).

4.2 Internal Stress Analysis

The picture below was taken from one of the samples using an angle where the light intensity was enough to see the fringes patterns clearly. It is possible to observe the patterns forming at the corners. This indicates a high concentration of stress in the corners.

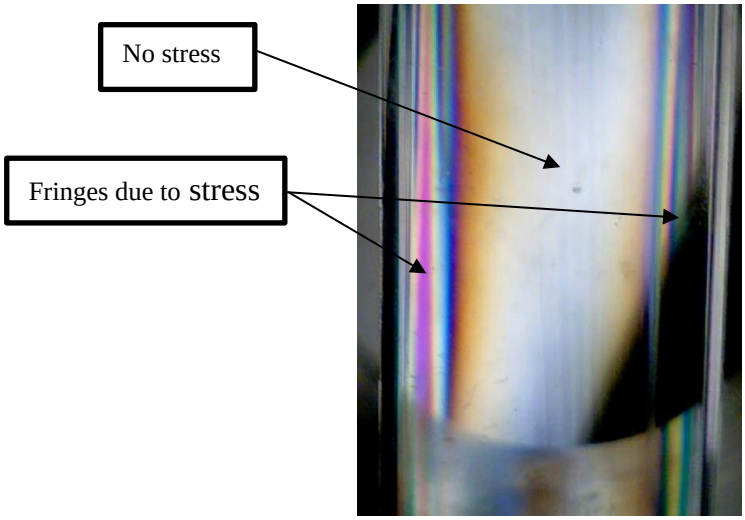

Figure 25: *Fringe patterns caused by internal stress in the PET sample. Arcada, 2018*

The following table shows a coloured picture from samples 1 to 10. The angles were chosen such as the least light intensity would come through the sample. This way the intensity is enough to reveal only the internal stress within the samples. Even though the images are somewhat dark, it is still possible to see the fringe patterns forming in the edges. The samples are in the same position (vertical) as the sample in the figure 32. Here the pictures are shown instead of the graphs because the location of the stress is wished to be seen. The graphs show us how big is the area affected with stress and the difference

in intensity due to induced stress. The graph does not show us the exact location of the stress.

Table 2: *Samples 1-10 internal stress and used angle. Arcada, 2018*

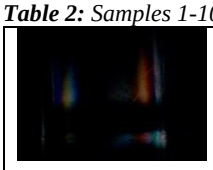	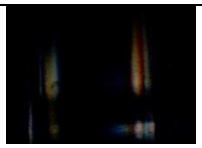			
#sample 1 (α + 1°)	#sample 2 (α + 2°)	#sample 3 (α + 2°)	#sample 4 (α + 0°)	#sample 5 (α + 2°)
			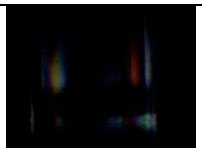	
#sample 6 (α + 0°)	#sample 7 (α + 1°)	#sample 8 (α + 0°)	#sample 9 (α + 0°)	#sample 10 (α + 0°)

4.3 Load Analysis

Here is presented the graphs obtained from the analysis made on samples 2, 7, and 8 undergoing different loads.

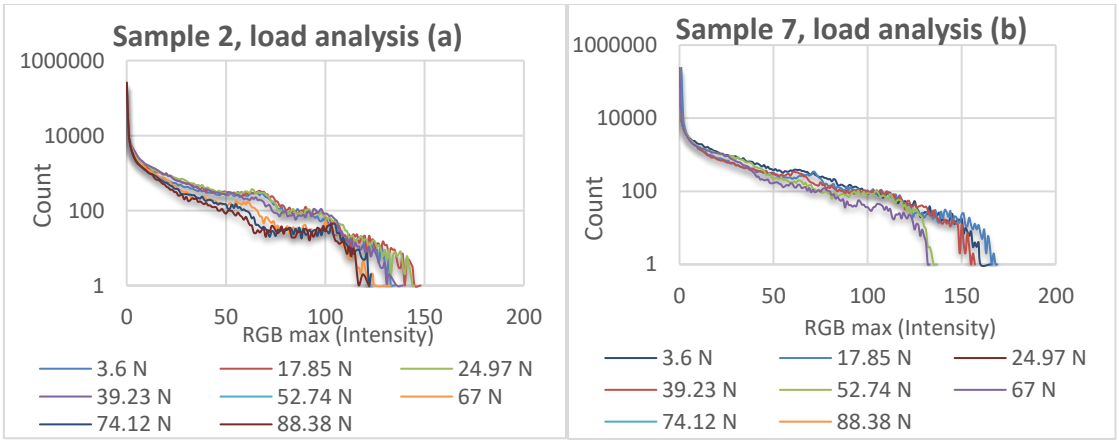

Figure 26a and 26b*: Sample 2 and 7, load analysis graph. Arcada, 2018*

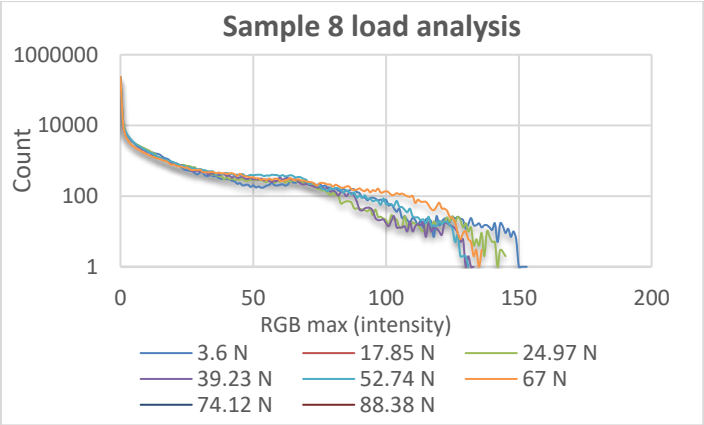

Figure 27: *Sample 8 load analysis graph. Arcada, 2018*

By observing the graphs, it is possible to see that samples 8 and 7 had the highest intensities (the minimum intensity is around 132 for sample 7 and 133 for sample 8). For the line representing the load of 17.85 N in figure 26b (sample 7) the intensity is around 166. In figure 27 (sample 8), the line representing the load of 3.6 N shows intensity around 150. When comparing the two samples, the data shows a higher intensity in sample 7, but more variations in the curves of sample 8. By comparing figure 26a (sample 2) and 27, it is possible to see more variation in the curves in the graph representing sample 2, however sample 8 has higher intensity. Based on these results, sample 8 was chosen to perform further investigation.

Sample 8 was analysed using an angle $\alpha + 0$. This can be seen from table 2. The angle chosen to analyse the internal stress of the samples was used for all the other analyses. The graphs show some variations due to external light. It was important then, to always use the same angle in all analyses. This way no confusion rises on what is causing the changes in the curve. Using always the same angle help us to know the difference between the changes caused by light interference and the changes caused by the load and thermal healing analysis.

When a load is applied, the stress in the sample will cause a $\sin^2$ change in intensity as described before. This means that the applied stress will disturb the $\sin^2$ curve, and it will have variations related to the picks where the highest light intensities are located. Below

it is shown the graph extracted from the data of the experiment described in section 4.1 presenting only the intensity coming from the polariscope at the angle α + 0 without a medium.

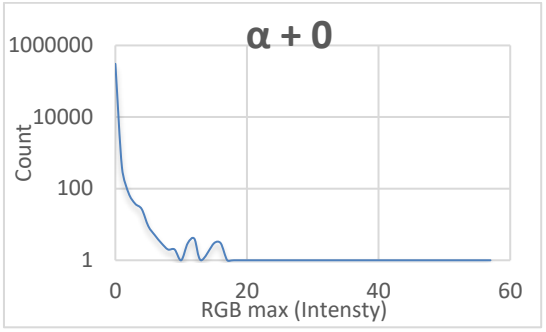

Figure 28: *Intensity of light at α + 0 angle. Arcada, 2018*

At this angle, it is expected the least amount light coming through the polariscope. This means that the intensity should be close to 0 and not close to 60 as shown in the graph. The variation in the graph is probably due to light interferences caused by other sources such as ambient light.

Below it is presented a separated graph for each load and stresses applied to sample 8. The graphs start from the coordinates which represent the intensity caused by the stress, therefore, eliminating the data information that comes from the empty parts located on the surroundings of the sample. The internal stress was included in all graphs. This way it is possible to observe the variations due to external stresses.

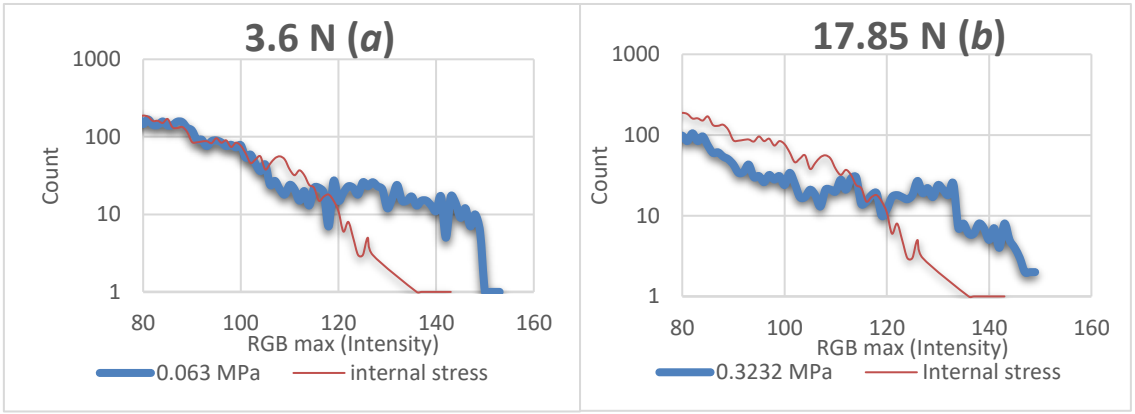

Figure 29a and 29b: *3.6 N load and 17.85 N load, sample 8. Arcada, 2018*

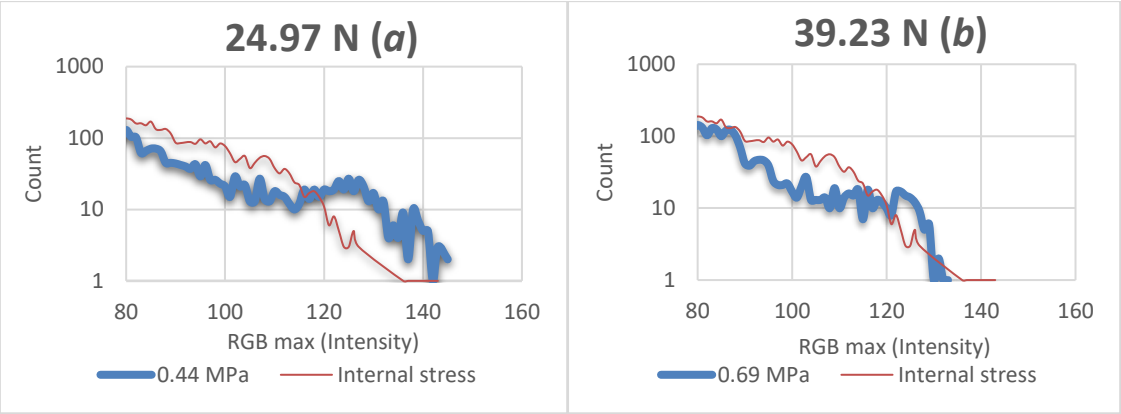

Figure 30a and 30b: *24.97 N and 39.23 N load, sample 8. Arcada, 2018*

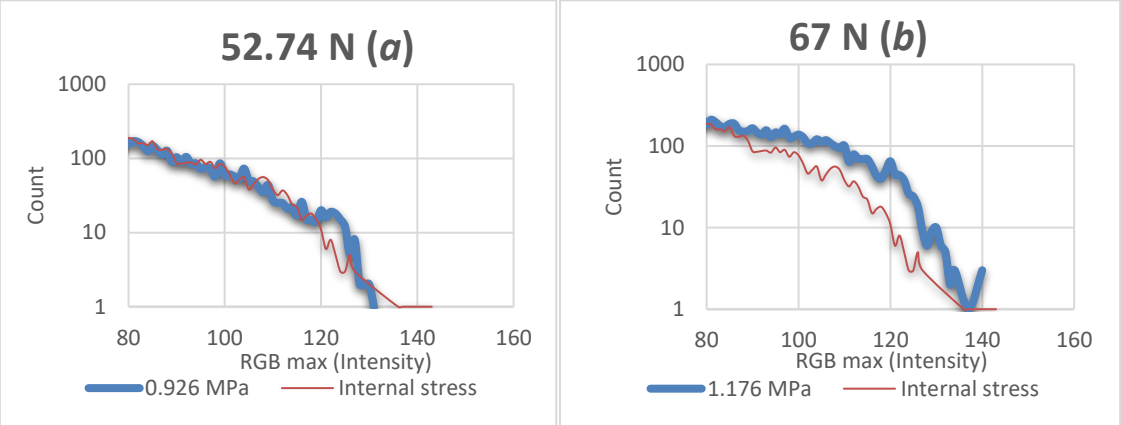

Figure 31a and 31b: *52.74 N and 67 N load, sample 8. Arcada, 2018*

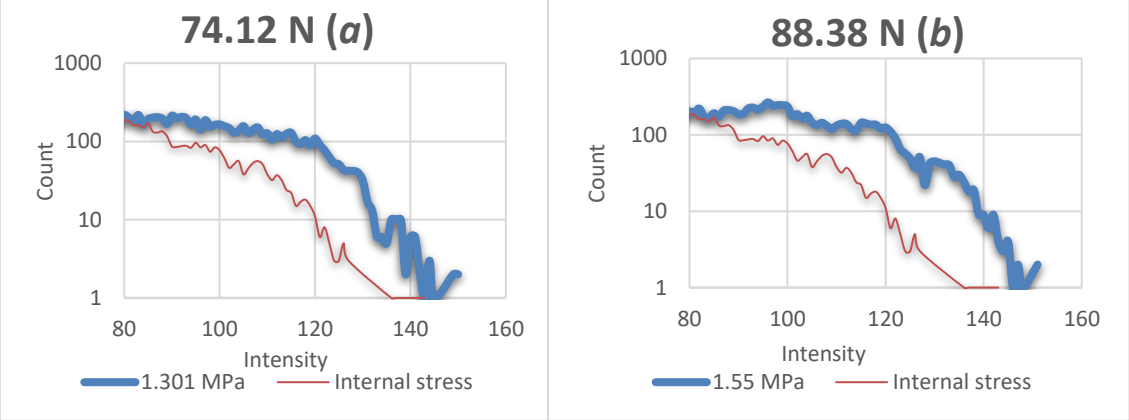

Figure 32a and 32b: *74.12 N and 88.38 N load, sample 8. Arcada, 2018*

It is possible to see that sometimes the induced stress curve appears lower than the internal stress curve. This is because the count axis represents the areas under stress. A lower

curve does not mean less stress, it just means that the location and area of the stress is different. It is possible to observe this from figures 29 *a* and *b* and 30 *a* and *b*. As the load increases and the stress becomes higher there is an increase of the areas under stress, but a decrease in intensity. To observe the changes in intensity due to induced stress, the difference between the maximum intensity caused by internal stress and the maximum intensity caused by the stress created by the loads was taken (Table 4 shows the values for intensity relating the internal stresses of each sample). The results are shown in table 3. From the table, a negative value is obtained at the stresses of 0.689 MPa, 0.93 MPa, and 1.18 MPa. This means that the maximum intensity of the induced stress is lower than the maximum intensity of the internal stress.

Table 3: *Stress calculation and maximum intensity difference. Arcada, 2018*

thickness	0.003	*m*	**mass in [kg]**	**Force in [N]**	**Stress [MPa]**	**Intensity**	**ΔI**
width	0.019	*m*	0.366	3.59046	0.06299053	153	10
			1.82	17.8542	0.31323158	149	6
area	0.000057	m^2	2.546	24.97626	0.43818	145	2
			4	39.24	0.68842105	133	-10
			5.378	52.75818	0.92558211	131	-12
			6.832	67.02192	1.17582316	140	-3
			7.558	74.14398	1.30077158	150	7
			9.012	88.40772	1.55101263	151	8

The stress was calculated using equation 1,

$$\sigma = \frac{F}{A} = \frac{mg}{A}$$

4.4 Thermal Healing Analysis

Below it is possible to observe the results obtained from thermal healing. First, it is presented the graphs representing the stress before the treatment (figures 33a, 34a, and 35a). Then, beside the internal stress graphs it is presented the graphs showing the results after the samples were treated 24 hours at 50°C and 24 four hours at 80°C (figures 33b, 34b and 35b).

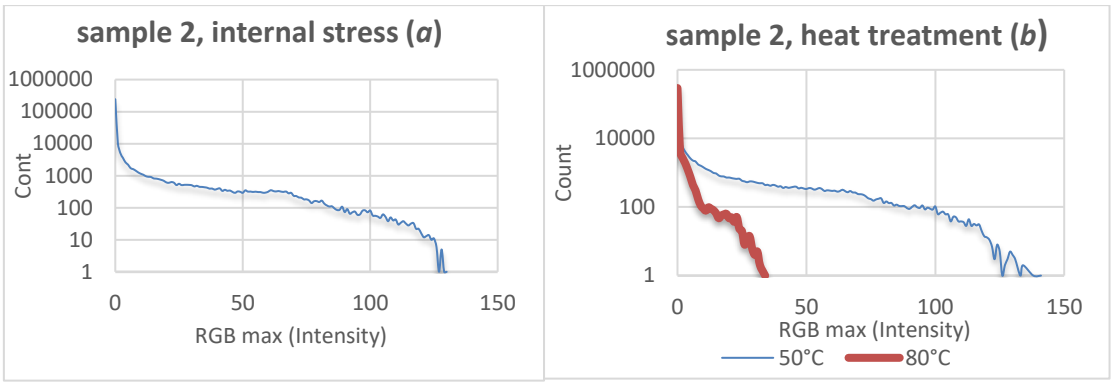

***Figure 33a and 33b**: Sample 2, internal stress and thermal healing graphs. Arcada, 2018*

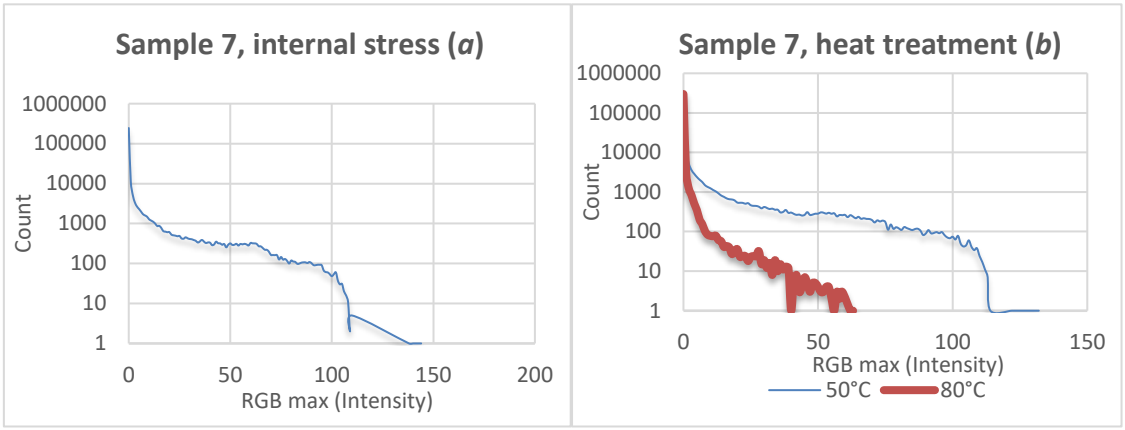

***Figure 34a and 34b:** Sample 7, internal stress and thermal healing graphs. Arcada, 2018*

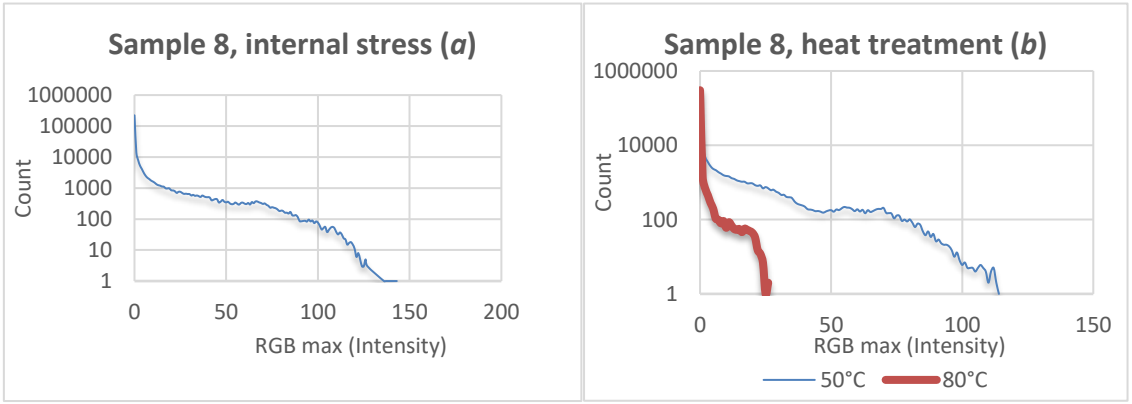

***Figure 35a and 35b:** Sample 7, internal stress and thermal healing graphs. Arcada, 2018*

The difference between the maximum internal intensity before and after the treatment was also calculated:

Table 4: *Thermal healing maximum intensity difference. Arcada, 2018*

	sample 2		**sample 7**		**sample 8**	
	Intensity (max)	ΔI	Intensity (max)	ΔI	Intensity (max)	ΔI
Internal stress	130		144		143	
50 °C	141	-11	132	12	114	29
80 °C	34	96	63	81	26	117

There is not a big variation after the samples were treated at 50 °C for 24 hours. It is possible to observe more of a stress distribution rather than a decrease in intensity. However, the samples have a drasticaly decrease of internal stress after treated at 80 °C for 24 hours. By observing table 4, one can see that the difference between the internal stress and the stress after the 80 °C treatment is significant. To demonstrate that what was said is true, below it is shown a coloured picure of the internal stresses of each sample after 80 °C treatment. There is almost no internal stress and only a small area with a little bit of green colour.

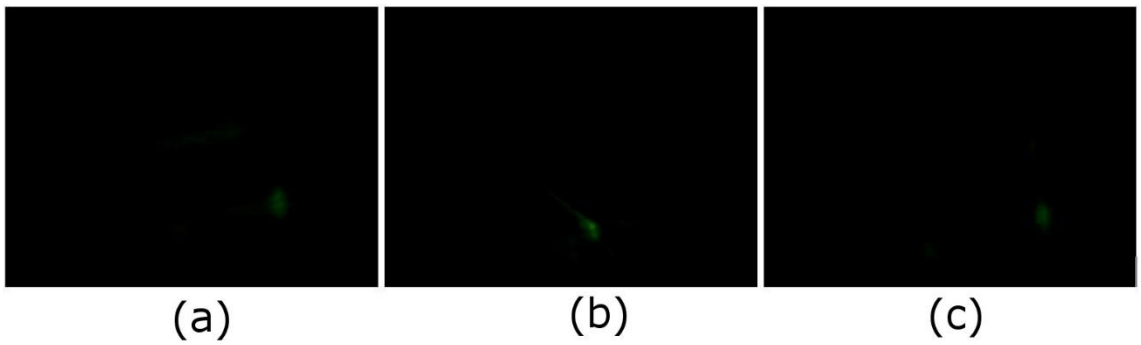

Figure 36a, 36b and 36c: *Internal stresses of samples 2, 7 and 8 after treatment. Arcada, 2018*

5 DISCUSSION

The method used in section 4.2, was made to allow us to observe where the internal stress is located in the samples. In the literature review chapter, it was described in the injection moulding subchapter that internal stress can occur due to shrinkage. Figure 25 represents clearly a defect caused during the IMP since no external load was applied to the sample. When internal stress is located such as at the area shown in figure 25 and on the figures from table 2, it is certain that the stress is due shrinkage when the sample was cooling. As described previously in this work, this is a result of setting the cooling time in the IMM wrong. The shrinkage happens when the cooling process is too slow. When cooling, the middle of the specimen has a uniform solidification, but the same cannot be said of the corners. If the time is too slow the outer parts of the sample will cool faster than the middle. This in turn cause the shrinkage in the corners, thus causing internal stress concentration.

On the results obtained from the load analysis it was presented that at certain loads the induced stress curve appears lower than the internal stress curve. When the curve representing the applied stress is located under the internal stress curve, the induced stress is relocating the internal stress to other areas of the sample. It was also shown that the intensity decreases as the stress increases. This could be related to the internal stress being removed from the samples when under higher loads. Since it is also shown that the area of stress increases with bigger loads, it also may well be that the stress is being distributed throughout the sample making it more uniform. The reason why the intensity is higher when the load is smaller might indicate that smaller loads do not cause big changes in the internal stress of the samples. When the load is small, it only creates more stress and relocates the internal stress to other areas.

In the thermal healing results, it can be seen from table 4 the difference of ΔI (maximum intensity) between the internal stress before and the internal stress after the samples were treated. There is no doubt that by keeping the samples at 80°C for 24 hours in the oven,

it was possible to decrease drastically the amount of stress. The internal stresses intensity values of samples 2, 7 and 8 before treatment were 130, 144 and 143 respectively. After the treatment the same samples 2, 7 and 8 had their stresses intensity values diminished to 34, 63 and 26 respectively. It is interesting to observe the line representing the thermal healing at 50°C in the graph of sample 2 (figure 33b). The sample has an increase in intensity after the heat treatment. It is only possible to speculate what caused this. It could have been due to shrinkage when the samples were removed from the oven or wrong setup of the equipment when analysing the sample again.

The objectives stated in the beginning of this work were achieved. It has been demonstrated that the samples suffered internal stress during processing. It was established that observing the stress using photoelasticity is possible. The analysis presented revealed that it is possible to extract data from the captured pictures, and that using these numbers one can see the stress variations within the material. The load and healing analysis verified that the average light intensity depends on the stress magnitude. It is possible to see this on the results obtained after the samples were treated at 80 °C. The intensity numbers have a significant decrease showing that it is indeed a result of stress decrease. The thermal healing also shows to be effective when relieving internal stress.

6 CONCLUSION

Most stress analysis methods show how a material will react under an applied force. These methods try to investigate the amount of stress which will cause the material to fail. Photoelasticity differs from these methods because it gives us information of the stress already existent on the surface and within the material. This is valuable information since these stresses are related to errors in processing and could also originate failure of the material.

The data analysis method described in this research gives us a quicker way to analyse the data from photoelastic analysis. If a software which creates a count-intensity graph directly from a picture would be developed, the process would be relatively fast. The graph is also useful when the stress in the material is small and the fringe patterns cannot be counted. As mentioned in the literature review section, a set of lines called isoclinic can obscure the fringe patterns causing confusion. With the graph analysis method this would not be a problem since the analysis deals with the light intensity data from a picture.

For the photoelastic stress analysis performed in this research a white light source was used. When using white light, data is registered from around the sample where there is only dark. Therefore, it is expected to obtain only a general qualitative assessment of the samples. Monochromatic sources are preferred when quantitative photoelastic measurements are needed. An example, would be to perform the analysis using laser source. This way, it is possible to focus the light in a point or particular position where it is wished to measure the stress, thus, providing us with an accurate result.

For further studies, it would be interesting to explore the possibility of using polarizing films to do photoelasticity analysis. This method is cheap and fast. A polarizing film of size around 10 x 10 cm, costs an average price of 15€, and the film can be used in non-transparent materials. This method is very simple, it is only needed to glue the film on to material to be analysed and then the sample is ready for testing.

7 REFERENCES

[1] J. W. Philips, “ApEfFotoelastico,” *Experimental Stress Analysis,* 17 Julho 2015.

[2] Vishay precision group, “PhotoStress instruments,” *Introduction to Stress Analysis by the PhotoStress Method,* 29 Jun 2011.

[3] V. Goodship, Troubleshooting Injection Moulding, vol. 15, Shrewsbury: iSmither Rapra Publishing, 2004.

[4] M. R. James, “Relaxation of Residual Stresses,” vol. 4, pp. 349-365, 1987.

[5] L. Tran, “Stress Concentration Analysis of Materials,” *Theseus,* 2016.

[6] V. Rodrigues, P. J. Herrera-Franco and P. I. Gonzáles-Chi, “Analysis of the interface between a thermoplastic fiber and a thermosetting matrix using photoelasticity,” *Composites Part A: Applied Science and Manufacturing,* vol. 38, no. 3, pp. 819-927, 2016.

[7] P. T. Nowak and J. L. Jankowski, “Application of photoelastic coating technique in tests of solid wooden beams reinforced with CFRP strips,” *Archives of Civil and Mechanical Engineering,* vol. 10, no. 2, pp. 53-66, 2012.

[8] J. Milch, “Digital image capture,” *How a picture can be represented as a collection of numbers,* 2015.

[9] Northeaster University, “Qualitative Research Methods: A Data Collector’s Field Guide,” *Qualitative Research Methods Overview*, pp. 1-12, 09 January 2012.

[10] R. C. Hibbeler, Mechanics of Materials, 9th ed., New Jersey: Pearson Prentice Hall, 2014.

[11] M. Kutz, Applied Plastics Engineering Handbook: Processing and Materials, Waltham: Elsevier Science &Technology, 2014.

[12] E. C. Carraher Jr, Introduction to Polymer Chemistry, 4th ed., Northwest Washington: Taylor & Francis group, 2017.

[13] S. N. Allen, Photochemistry and Photophysics of Polymeric Materials, 1 ed., New Jersey: Wiley, 2010.

[14] B. Demirel, A. Yaras and H. Elçiçek, “Crystallization Behavior of PET Materials,” *BAÜ Fen Bil. Enst. Dergisi Cilt,* vol. 13, no. 1, pp. 26-35, 2011.

[15] W. Schnabel, Polymers and Electromagnetic Radiation, 1st ed., Weinheim: John Wiley & Sons, Incorporated, 2014.

[16] A. Shukla, Dynamic Fracture Mechanics, Singapore: World Scientific Publishing Co Pte Ltd, 2006.

[17] E. J. Hern, Mechanics of Materials 2: The mechanics of Elastic and Plastic Deformations of Solids and Structural Materials, 3rd ed., Oxford: Elsevier Science & Technology, 1997.

[18] R. E. Newnham, Properties of Materials: Ansiotopry, Symetry, Structure, Oxford : OUP Oxford, 2005.

[19] F. J. Doyle, D. J. Philips and D. Post, Manual on Experimental Stress Analysis, 5th ed., Society for experimental Mechanics, 1989.

[20] G. Stark, "Light-Physics," *optical spectrum, visible radiation, visible spectrum,* pp. 1-10, 2 February 2018.

[21] G. Elert, "The Nature Of Light," in *The Physics*, New York , 2018.

[22] Encyclopaedia Britannica, "Frequency-Physics," 2018.

[23] Encyclopaedia Britannica, "Refraction-Physics," 15 January 2018.

[24] A. C. Sciammarella and M. A. Sciammarella, Experimental Mechanics of Solids, 1st ed., Chischester: John Wiley & Sons, 2012.

[25] Encyclopaedia Britannica, “Refractive Index-Physics,” 2018.

[26] K. P. Burian, Imaging, Mastering Digital Photography and Imaging, 1st ed., Wiley, 2005.

[27] C. Salvaggio, “Digital Image Capture,” *What is Inside a JPEG File,* 2015.

APPENDIX I

Analysis without a medium data. Pictures in black and white. Arcada, 2018

α + 90		α + 80		α + 70		α + 60		α + 50		α + 40		α + 30		α + 20		α + 10		α + 0	
0	54041	0	74161	0	97013	0	136097	0	193407	0	249823	0	260888	0	294694	0	306556	0	306623
1	7890	1	11056	1	15209	1	13569	1	7311	1	7202	1	10626	1	5973	1	429	1	393
2	4718	2	6704	2	6929	2	6038	2	4695	2	4271	2	6273	2	2673	2	85	2	76
3	4338	3	5659	3	5673	3	4605	3	3736	3	3255	3	5201	3	1651	3	40	3	38
4	4356	4	4940	4	4806	4	3900	4	3221	4	2746	4	4285	4	1023	4	37	4	27
5	4068	5	4252	5	4050	5	3431	5	2902	5	2469	5	3376	5	599	5	12	5	9
6	3984	6	3905	6	3654	6	3109	6	2513	6	2134	6	3060	6	312	6	10	6	5
7	3650	7	3596	7	3417	7	2788	7	2372	7	1955	7	2637	7	148	7	5	7	3
8	3489	8	3394	8	3133	8	2720	8	2102	8	1814	8	2215	8	58	8	1	8	2
9	3272	9	3129	9	2638	9	2455	9	1935	9	1709	9	1768	9	30	9	4	9	2
10	3101	10	2867	10	2640	10	2425	10	1888	10	1593	10	1472	10	12	10	3	10	1
11	3032	11	2810	11	2559	11	2276	11	1753	11	1450	11	1143	11	6	11	4	11	3
12	2727	12	2650	12	2375	12	2184	12	1770	12	1363	12	1036	12	4	12	1	12	4
13	2689	13	2537	13	2170	13	2178	13	1621	13	1365	13	784	13	4	14	1	13	1
14	2714	14	2464	14	2040	14	2042	14	1538	14	1280	14	658	14	2	15	2	15	3
15	2621	15	2397	15	2146	15	1937	15	1556	15	1283	15	472	15	1	18	2	16	3
16	2683	16	2355	16	2029	16	1735	16	1505	16	1213	16	389	16	2	21	1	17	1
17	2680	17	2179	17	2108	17	1657	17	1517	17	1210	17	268	17	1	22	1	18	1
18	2564	18	2194	18	1917	18	1588	18	1510	18	1208	18	196	20	1	24	1	23	1
19	2376	19	2145	19	1943	19	1647	19	1450	19	1086	19	147	22	1	31	1	25	1
20	2268	20	2162	20	1904	20	1586	20	1449	20	1117	20	115	30	1	33	1	55	1
21	2241	21	2090	21	1761	21	1627	21	1350	21	1105	21	71	32	1	53	1	56	1
22	2249	22	1955	22	1774	22	1559	22	1359	22	1037	22	49	57	1	56	2	57	1
23	2294	23	1881	23	1804	23	1580	23	1310	23	1015			59	1	23	26		
24	2222	24	1745	24	1720	24	1557	24	1332	24	999			62	1	24	19		
25	2163	25	1776	25	1716	25	1530	25	1283	25	1004					25	9		
26	2119	26	1657	26	1721	26	1444	26	1278	26	979					26	4		
27	2050	27	1638	27	1654	27	1380	27	1298	27	923					27	8		
28	1965	28	1612	28	1598	28	1366	28	1276	28	945					31	1		
29	1994	29	1577	29	1533	29	1265	29	1293	29	907					32	1		
30	1948	30	1601	30	1415	30	1268	30	1316	30	807					46	1		
31	1827	31	1618	31	1378	31	1287	31	1272	31	817					52	2		
32	1725	32	1484	32	1378	32	1294	32	1196	32	659								
33	1637	33	1522	33	1327	33	1295	33	1172	33	594								
34	1645	34	1450	34	1368	34	1212	34	1112	34	563								
35	1595	35	1409	35	1332	35	1137	35	1094	35	529								
36	1592	36	1349	36	1216	36	1142	36	1101	36	454								
37	1525	37	1336	37	1258	37	1162	37	1127	37	357								
38	1522	38	1266	38	1145	38	1102	38	1097	38	328								
39	1395	39	1245	39	1150	39	1082	39	1085	39	337								
40	1347	40	1253	40	1108	40	1099	40	1031	40	274								
41	1311	41	1269	41	1128	41	1073	41	1029	41	233								
42	1376	42	1259	42	1060	42	1031	42	1029	42	191								
43	1304	43	1285	43	1043	43	1075	43	936	43	141								
44	1260	44	1167	44	1117	44	978	44	905	44	118								
45	1208	45	1126	45	1049	45	898	45	962	45	97								
46	1205	46	1082	46	1047	46	979	46	885	46	71								
47	1213	47	1092	47	1037	47	893	47	953	47	36								
48	1204	48	1093	48	1059	48	887	48	912	48	36								
49	1205	49	1057	49	1090	49	861	49	886	49	28								
50	1148	50	1035	50	999	50	862	50	857	50	18								
51	1224	51	1018	51	970	51	886	51	878	51	10								
52	1178	52	1077	52	1008	52	820	52	847	52	11								
53	1124	53	1045	53	1028	53	872	53	841	53	11								
54	1183	54	1061	54	1014	54	908	54	782	54	4								
55	1145	55	1149	55	962	55	956	55	820	55	2								
56	1298	56	1149	56	1062	56	1002	56	845	56	2								
57	1382	57	1225	57	1152	57	1014	57	860	57	1								
58	1385	58	1381	58	1195	58	1168	58	861	58	1								
59	1493	59	1552	59	1313	59	1176	59	969	59	1								
60	1622	60	1622	60	1387	60	1311	60	1020	60	1								
61	1789	61	1649	61	1599	61	1437	61	1085	61	3								
62	1875	62	1659	62	1573	62	1526	62	1137	63	1								

63	1955	63	1740	63	1684	63	1589	63	1195	64	1
64	2000	64	1722	64	1701	64	1593	64	1199	65	2
65	1975	65	1875	65	1590	65	1604	65	1238	67	1
66	1892	66	1863	66	1618	66	1635	66	1158		
67	1917	67	1758	67	1664	67	1606	67	1207		
68	1698	68	1650	68	1592	68	1630	68	1226		
69	1764	69	1636	69	1460	69	1548	69	1244		
70	1607	70	1397	70	1440	70	1557	70	1224		
71	1617	71	1401	71	1440	71	1505	71	1134		
72	1474	72	1437	72	1369	72	1476	72	1189		
73	1410	73	1312	73	1303	73	1420	73	1055		
74	1266	74	1172	74	1179	74	1317	74	981		
75	1254	75	1090	75	1158	75	1237	75	845		
76	1283	76	1075	76	1105	76	1170	76	814		
77	1304	77	1064	77	1227	77	1171	77	670		
78	1335	78	1171	78	1250	78	1103	78	606		
79	1337	79	1170	79	1122	79	1195	79	569		
80	1366	80	1104	80	1141	80	1227	80	523		
81	1317	81	1222	81	1187	81	1104	81	461		
82	1298	82	1212	82	1117	82	1034	82	444		
83	1200	83	1187	83	1115	83	1004	83	472		
84	1131	84	1211	84	1204	84	975	84	433		
85	1139	85	1149	85	1161	85	971	85	286		
86	1129	86	1111	86	1198	86	927	86	176		
87	1132	87	1138	87	1206	87	882	87	129		
88	1143	88	1112	88	1090	88	943	88	98		
89	1101	89	1184	89	1156	89	981	89	67		
90	1193	90	1123	90	1210	90	982	90	47		
91	1247	91	1211	91	1269	91	983	91	37		
92	1199	92	1268	92	1348	92	1040	92	18		
93	1257	93	1164	93	1319	93	979	93	11		
94	1280	94	1197	94	1233	94	1017	94	5		
95	1176	95	1197	95	1232	95	1123	95	6		
96	1152	96	1173	96	1251	96	1024	97	1		
97	1083	97	1175	97	1141	97	979				
98	1066	98	1256	98	1029	98	971				
99	1083	99	1188	99	1002	99	912				
100	1092	100	1252	100	1041	100	904				
101	1023	101	1267	101	1013	101	906				
102	1038	102	1224	102	1103	102	859				
103	1039	103	1160	103	988	103	801				
104	1011	104	1210	104	952	104	741				
105	1088	105	1143	105	981	105	692				
106	1060	106	1053	106	910	106	748				
107	1017	107	1080	107	924	107	730				
108	940	108	1054	108	943	108	713				
109	1071	109	1056	109	849	109	709				
110	1031	110	1041	110	817	110	653				
111	1049	111	1051	111	814	111	527				
112	1005	112	1097	112	782	112	558				
113	984	113	1044	113	802	113	559				
114	1031	114	1085	114	737	114	552				
115	1086	115	963	115	813	115	447				
116	1063	116	1017	116	897	116	412				
117	1206	117	1008	117	921	117	379				
118	1148	118	1118	118	909	118	403				
119	1250	119	1035	119	923	119	427				
120	1307	120	1091	120	999	120	370				
121	1252	121	1042	121	1023	121	239				
122	1192	122	973	122	985	122	136				
123	1072	123	937	123	1004	123	108				
124	1030	124	908	124	956	124	67				
125	982	125	830	125	808	125	53				
126	944	126	839	126	744	126	52				

127	941	127	758	127	637	127	41
128	812	128	773	128	693	128	12
129	785	129	732	129	638	129	13
130	906	130	768	130	606	130	7
131	856	131	789	131	590		
132	930	132	831	132	661		
133	954	133	823	133	663		
134	909	134	875	134	590		
135	958	135	775	135	537		
136	924	136	809	136	604		
137	827	137	782	137	565		
138	785	138	754	138	457		
139	768	139	812	139	441		
140	727	140	822	140	365		
141	727	141	816	141	286		
142	793	142	884	142	280		
143	833	143	784	143	330		
144	803	144	770	144	295		
145	806	145	695	145	248		
146	857	146	714	146	169		
147	814	147	752	147	141		
148	823	148	738	148	92		
149	831	149	662	149	77		
150	870	150	618	150	68		
151	710	151	605	151	52		
152	749	152	499	152	77		
153	644	153	486	153	66		
154	619	154	498	154	82		
155	698	155	519	155	47		
156	762	156	471	156	54		
157	753	157	469	157	33		
158	755	158	401	158	6		
159	777	159	377				
160	896	160	311				
161	939	161	239				
162	916	162	170				
163	785	163	103				
164	718	164	87				
165	747	165	69				
166	593	166	65				
167	557	167	76				
168	624	168	89				
169	552	169	115				
170	596	170	101				
171	507	171	88				
172	432	172	44				
173	357	173	15				
174	342	174	2				
175	266						
176	248						
177	235						
178	225						
179	133						
180	124						
181	105						
182	85						
183	62						
184	36						
185	50						
186	39						
187	29						
188	22						
189	14						
190	19						
191	2						

Internal sterss analysis data. Samples 1 to 10, pictures in black and white. Arcada, 2018

	sample 1		sample 2		sampl 3		sample 4		sample 5		sample 6		sample 7		sample 8		sample 9		sample 10
0	240208	0	243719	0	238713	0	249276	0	257374	0	250498	0	245911	0	222740	0	251994	0	241944
1	11442	1	10704	1	12051	1	9923	1	10098	1	10664	1	11097	1	14004	1	10033	1	10969
2	5557	2	5048	2	5990	2	4729	2	4370	2	4737	2	5129	2	7918	2	4825	2	5453
3	4087	3	3601	3	3843	3	3371	3	3013	3	3211	3	3388	3	5314	3	3506	3	3888
4	3301	4	2611	4	2875	4	2656	4	2198	4	2536	4	2688	4	4137	4	2634	4	3078
5	2665	5	2217	5	2283	5	2193	5	1755	5	2038	5	2330	5	3147	5	2228	5	2682
6	2324	6	1722	6	1939	6	1884	6	1467	6	1798	6	2007	6	2528	6	1980	6	2320
7	2095	7	1606	7	1724	7	1692	7	1380	7	1559	7	1716	7	2165	7	1766	7	2145
8	1945	8	1440	8	1546	8	1589	8	1166	8	1441	8	1595	8	1967	8	1594	8	1876
9	1788	9	1267	9	1417	9	1398	9	1034	9	1254	9	1488	9	1752	9	1421	9	1694
10	1656	10	1150	10	1319	10	1276	10	956	10	1178	10	1280	10	1625	10	1244	10	1626
11	1617	11	1071	11	1199	11	1196	11	849	11	1040	11	1189	11	1488	11	1108	11	1555
12	1444	12	965	12	1132	12	1124	12	774	12	988	12	1110	12	1326	12	1009	12	1384
13	1389	13	924	13	1017	13	964	13	737	13	939	13	1001	13	1239	13	968	13	1373
14	1329	14	914	14	1023	14	938	14	707	14	800	14	868	14	1196	14	923	14	1265
15	1232	15	825	15	946	15	860	15	654	15	768	15	876	15	1121	15	839	15	1185
16	1159	16	812	16	849	16	865	16	578	16	748	16	780	16	1111	16	730	16	1072
17	1012	17	782	17	771	17	811	17	601	17	701	17	646	17	980	17	733	17	1034
18	979	18	742	18	756	18	703	18	558	18	634	18	629	18	974	18	650	18	971
19	880	19	695	19	675	19	738	19	513	19	624	19	608	19	981	19	686	19	910
20	797	20	619	20	652	20	646	20	515	20	593	20	612	20	849	20	610	20	796
21	744	21	599	21	588	21	609	21	458	21	560	21	527	21	839	21	586	21	744
22	672	22	634	22	532	22	644	22	479	22	548	22	509	22	793	22	545	22	765
23	668	23	605	23	549	23	593	23	480	23	533	23	498	23	697	23	488	23	674
24	557	24	510	24	526	24	530	24	453	24	502	24	482	24	758	24	521	24	648
25	524	25	560	25	508	25	530	25	384	25	496	25	489	25	758	25	522	25	634
26	504	26	509	26	491	26	506	26	405	26	462	26	425	26	696	26	504	26	562
27	488	27	518	27	470	27	512	27	404	27	496	27	418	27	649	27	464	27	567
28	460	28	520	28	398	28	444	28	371	28	450	28	453	28	660	28	415	28	535
29	457	29	516	29	405	29	439	29	354	29	418	29	427	29	642	29	392	29	478
30	426	30	505	30	367	30	407	30	405	30	391	30	411	30	642	30	358	30	474
31	398	31	463	31	396	31	410	31	401	31	399	31	405	31	575	31	373	31	435
32	418	32	484	32	368	32	373	32	338	32	370	32	387	32	604	32	386	32	443
33	375	33	450	33	349	33	373	33	337	33	340	33	370	33	561	33	373	33	408
34	351	34	447	34	344	34	328	34	336	34	333	34	335	34	577	34	357	34	358
35	353	35	436	35	347	35	355	35	333	35	318	35	356	35	551	35	294	35	386
36	354	36	423	36	335	36	305	36	320	36	287	36	391	36	517	36	352	36	345
37	333	37	395	37	340	37	308	37	310	37	304	37	355	37	576	37	298	37	345
38	322	38	398	38	340	38	319	38	317	38	290	38	325	38	535	38	298	38	293
39	315	39	367	39	338	39	275	39	328	39	269	39	337	39	511	39	301	39	315
40	296	40	388	40	328	40	308	40	270	40	275	40	333	40	509	40	312	40	284
41	311	41	402	41	344	41	270	41	255	41	287	41	289	41	498	41	270	41	280
42	343	42	335	42	313	42	273	42	273	42	257	42	299	42	405	42	277	42	294
43	308	43	363	43	312	43	284	43	288	43	228	43	352	43	418	43	227	43	279
44	311	44	338	44	320	44	245	44	266	44	250	44	321	44	443	44	261	44	282
45	318	45	345	45	318	45	226	45	288	45	258	45	320	45	435	45	192	45	251
46	332	46	311	46	297	46	249	46	280	46	254	46	294	46	343	46	244	46	233
47	367	47	292	47	268	47	226	47	267	47	251	47	308	47	366	47	183	47	263
48	342	48	323	48	278	48	250	48	270	48	264	48	254	48	413	48	198	48	232
49	336	49	314	49	281	49	260	49	243	49	257	49	296	49	362	49	184	49	205
50	330	50	292	50	290	50	258	50	249	50	249	50	319	50	346	50	197	50	230
51	398	51	349	51	305	51	242	51	292	51	264	51	292	51	362	51	198	51	250
52	346	52	319	52	278	52	225	52	286	52	259	52	295	52	320	52	190	52	247
53	299	53	320	53	342	53	198	53	247	53	243	53	311	53	302	53	179	53	232
54	313	54	311	54	327	54	203	54	236	54	245	54	282	54	309	54	207	54	241
55	294	55	317	55	320	55	243	55	224	55	237	55	309	55	342	55	183	55	234
56	286	56	309	56	335	56	222	56	237	56	255	56	301	56	313	56	190	56	248
57	295	57	308	57	344	57	250	57	239	57	245	57	311	57	292	57	213	57	215
58	243	58	293	58	376	58	227	58	258	58	238	58	300	58	330	58	209	58	218
59	255	59	297	59	348	59	273	59	256	59	257	59	283	59	340	59	230	59	216
60	233	60	317	60	386	60	275	60	239	60	271	60	327	60	315	60	235	60	185
61	225	61	354	61	385	61	270	61	258	61	248	61	320	61	305	61	201	61	194
62	267	62	332	62	374	62	274	62	241	62	245	62	319	62	330	62	244	62	196
63	251	63	322	63	364	63	291	63	247	63	270	63	310	63	295	63	226	63	190
64	222	64	332	64	416	64	284	64	245	64	250	64	271	64	354	64	222	64	204
65	218	65	319	65	386	65	273	65	203	65	250	65	269	65	327	65	231	65	173
66	193	66	312	66	351	66	271	66	208	66	268	66	244	66	371	66	208	66	176
67	197	67	321	67	388	67	248	67	179	67	249	67	221	67	368	67	211	67	143
68	146	68	282	68	371	68	210	68	171	68	226	68	220	68	344	68	194	68	131
69	142	69	292	69	380	69	203	69	176	69	232	69	198	69	330	69	208	69	134
70	117	70	235	70	333	70	162	70	159	70	194	70	164	70	308	70	171	70	124
71	103	71	232	71	316	71	188	71	115	71	185	71	163	71	320	71	162	71	97
72	94	72	209	72	290	72	138	72	112	72	163	72	162	72	287	72	164	72	93

73	94	73	206	73	283	73	123	73	115	73	153	73	162	73	268	73	136	73	98
74	71	74	182	74	274	74	128	74	85	74	146	74	126	74	232	74	107	74	86
75	64	75	183	75	240	75	110	75	99	75	140	75	146	75	242	75	94	75	76
76	66	76	169	76	256	76	101	76	73	76	118	76	125	76	232	76	98	76	94
77	44	77	140	77	224	77	87	77	66	77	120	77	130	77	223	77	63	77	79
78	59	78	160	78	203	78	70	78	75	78	117	78	116	78	204	78	53	78	72
79	49	79	161	79	165	79	103	79	62	79	112	79	100	79	181	79	38	79	85
80	31	80	151	80	173	80	74	80	58	80	114	80	119	80	188	80	34	80	78
81	34	81	167	81	167	81	81	81	62	81	88	81	112	81	182	81	20	81	68
82	29	82	134	82	129	82	93	82	50	82	104	82	110	82	160	82	24	82	74
83	34	83	118	83	116	83	78	83	47	83	82	83	98	83	161	83	13	83	68
84	22	84	109	84	128	84	58	84	42	84	83	84	100	84	151	84	17	84	66
85	23	85	111	85	110	85	79	85	28	85	68	85	105	85	170	85	10	85	78
86	36	86	95	86	127	86	73	86	14	86	58	86	107	86	133	86	17	86	43
87	16	87	85	87	127	87	66	87	13	87	60	87	107	87	130	87	14	87	53
88	14	88	86	88	94	88	61	88	3	88	54	88	103	88	134	88	18	88	36
89	7	89	108	89	99	89	56	89	5	89	55	89	109	89	116	89	20	89	34
90	12	90	73	90	96	90	56	90	4	90	64	90	102	90	86	90	14	90	42
91	14	91	91	91	102	91	69	91	5	91	68	91	91	91	85	91	14	91	34
92	15	92	65	92	92	92	69	92	1	92	60	92	91	92	87	92	13	92	27
93	15	93	72	93	77	93	73	93	1	93	56	93	93	93	88	93	11	93	25
94	8	94	76	94	110	94	64	94	2	94	53	94	93	94	83	94	5	94	21
95	7	95	60	95	109	95	56	120	1	95	51	95	91	95	96	95	10	95	22
96	7	96	62	96	84	96	58	123	1	96	53	96	67	96	84	96	7	96	20
97	9	97	81	97	91	97	59	130	1	97	59	97	61	97	90	97	1	97	19
98	7	98	83	98	95	98	48			98	61	98	60	98	74	98	5	98	15
99	9	99	72	99	94	99	35			99	43	99	54	99	84	99	4	99	30
100	8	100	82	100	75	100	17			100	51	100	48	100	77	100	4	100	13
101	11	101	57	101	83	101	16			101	38	101	54	101	61	101	1	101	14
102	7	102	56	102	113	102	12			102	25	102	60	102	46	103	2	102	13
103	8	103	53	103	74	103	5			103	30	103	37	103	51	104	1	103	14
104	2	104	48	104	72	104	2			104	31	104	30	104	56	109	2	104	7
105	6	105	62	105	77	105	2			105	30	105	31	105	38	113	1	105	14
107	2	106	52	106	67	106	4			106	27	106	20	106	45			106	5
109	1	107	38	107	68	107	1			107	22	107	16	107	53			107	10
110	1	108	50	108	51	108	1			108	15	108	11	108	56			108	7
111	1	109	40	109	43	113	1			109	8	109	2	109	51			109	9
113	1	110	43	110	41					110	5	110	5	110	38			110	15

Sample 2 load analysis data. Pictures in black and white. Arcada, 2018

sampe 2, 3.6 N		sample 2, 17.85 N		sample 2, 24.97 N		sample 2, 39.23 N		sample 2, 52.74 N		sample 2, 67 N		sample 2, 74.12 N		sample 2, 88.38	
0	246982	0	238118	0	233303	0	234621	0	241358	0	250777	0	256913	0	261307
1	9393	1	10432	1	11996	1	10190	1	11266	1	12481	1	11786	1	11289
2	4749	2	5058	2	5395	2	6323	2	5889	2	5783	2	5149	2	4989
3	3453	3	3585	3	3836	3	4715	3	4341	3	3902	3	3495	3	3148
4	2791	4	2926	4	3081	4	3880	4	3578	4	2831	4	2563	4	2378
5	2385	5	2532	5	2699	5	3150	5	2993	5	2317	5	2053	5	1908
6	2061	6	2121	6	2365	6	2598	6	2493	6	2044	6	1755	6	1690
7	1751	7	1934	7	2083	7	2264	7	2127	7	1796	7	1551	7	1529
8	1658	8	1734	8	1792	8	2070	8	1893	8	1555	8	1363	8	1403
9	1389	9	1655	9	1725	9	1817	9	1669	9	1446	9	1223	9	1286
10	1379	10	1550	10	1672	10	1682	10	1525	10	1277	10	1129	10	1151
11	1269	11	1365	11	1505	11	1592	11	1419	11	1193	11	1014	11	1014
12	1138	12	1340	12	1389	12	1502	12	1287	12	1084	12	940	12	967
13	1076	13	1255	13	1217	13	1411	13	1213	13	1044	13	927	13	889
14	975	14	1165	14	1226	14	1343	14	1168	14	940	14	867	14	735
15	871	15	1062	15	1134	15	1247	15	1092	15	913	15	801	15	668
16	766	16	1053	16	1095	16	1162	16	1010	16	818	16	732	16	652
17	747	17	1010	17	1031	17	1066	17	931	17	768	17	657	17	595
18	748	18	924	18	983	18	993	18	973	18	762	18	629	18	523
19	718	19	922	19	930	19	925	19	900	19	737	19	568	19	498
20	636	20	898	20	964	20	983	20	852	20	660	20	548	20	436
21	572	21	841	21	849	21	837	21	836	21	610	21	507	21	407
22	588	22	823	22	871	22	842	22	764	22	572	22	462	22	360
23	539	23	762	23	813	23	737	23	732	23	475	23	441	23	361
24	547	24	682	24	763	24	681	24	644	24	470	24	389	24	313
25	528	25	691	25	733	25	637	25	658	25	433	25	379	25	308
26	469	26	639	26	692	26	611	26	629	26	348	26	370	26	251
27	493	27	610	27	690	27	604	27	566	27	353	27	294	27	257
28	448	28	552	28	707	28	578	28	525	28	327	28	278	28	256
29	422	29	559	29	661	29	545	29	529	29	315	29	271	29	199
30	426	30	511	30	624	30	539	30	459	30	316	30	276	30	233
31	429	31	523	31	571	31	522	31	469	31	284	31	266	31	179
32	388	32	496	32	540	32	491	32	415	32	237	32	268	32	189
33	389	33	485	33	534	33	441	33	400	33	224	33	256	33	214
34	363	34	437	34	521	34	423	34	382	34	218	34	257	34	202
35	347	35	421	35	470	35	432	35	331	35	223	35	225	35	208
36	330	36	390	36	483	36	417	36	309	36	217	36	217	36	170
37	354	37	365	37	450	37	357	37	275	37	204	37	211	37	176
38	323	38	414	38	481	38	342	38	288	38	231	38	236	38	160
39	343	39	380	39	413	39	350	39	260	39	227	39	194	39	148
40	303	40	316	40	404	40	375	40	232	40	206	40	181	40	160
41	300	41	381	41	411	41	351	41	232	41	185	41	194	41	138
42	300	42	329	42	363	42	340	42	210	42	203	42	191	42	138
43	292	43	317	43	366	43	321	43	189	43	189	43	184	43	124
44	291	44	335	44	345	44	312	44	202	44	187	44	157	44	124
45	269	45	311	45	312	45	305	45	197	45	175	45	162	45	123
46	265	46	312	46	332	46	302	46	190	46	160	46	144	46	101
47	262	47	312	47	333	47	286	47	168	47	153	47	157	47	100
48	320	48	279	48	285	48	282	48	201	48	143	48	153	48	111
49	276	49	324	49	298	49	278	49	168	49	148	49	149	49	91
50	262	50	314	50	302	50	274	50	162	50	142	50	145	50	83
51	255	51	285	51	299	51	314	51	175	51	138	51	112	51	99
52	272	52	310	52	284	52	297	52	168	52	161	52	113	52	99
53	275	53	291	53	297	53	297	53	172	53	139	53	145	53	98
54	244	54	303	54	272	54	280	54	152	54	135	54	117	54	82
55	253	55	294	55	296	55	267	55	164	55	179	55	149	55	74
56	253	56	312	56	300	56	265	56	182	56	161	56	118	56	89
57	228	57	295	57	287	57	252	57	174	57	155	57	124	57	75
58	244	58	309	58	297	58	234	58	170	58	144	58	104	58	68
59	270	59	250	59	305	59	203	59	184	59	167	59	108	59	57
60	251	60	294	60	329	60	210	60	165	60	146	60	98	60	68
61	247	61	274	61	311	61	202	61	159	61	174	61	94	61	53
62	272	62	305	62	294	62	191	62	179	62	152	62	83	62	41
63	300	63	288	63	371	63	222	63	161	63	122	63	62	63	40
64	288	64	290	64	347	64	205	64	151	64	120	64	66	64	26
65	301	65	301	65	279	65	225	65	148	65	109	65	42	65	25
66	287	66	322	66	310	66	191	66	135	66	93	66	42	66	30
67	258	67	338	67	302	67	193	67	142	67	71	67	37	67	26
68	294	68	307	68	296	68	185	68	144	68	68	68	34	68	30
69	263	69	318	69	296	69	167	69	133	69	46	69	37	69	33
70	230	70	278	70	278	70	129	70	110	70	66	70	32	70	20
71	220	71	268	71	252	71	138	71	121	71	63	71	27	71	30
72	198	72	217	72	211	72	138	72	119	72	52	72	20	72	27

73	178	73	243	73	173	73	105	73	109	73	47	73	28	73	39
74	144	74	222	74	172	74	90	74	82	74	52	74	27	74	36
75	147	75	178	75	148	75	86	75	103	75	33	75	21	75	29
76	115	76	173	76	105	76	82	76	79	76	40	76	31	76	25
77	108	77	134	77	102	77	70	77	84	77	32	77	28	77	28
78	128	78	139	78	93	78	88	78	99	78	30	78	30	78	38
79	84	79	134	79	76	79	89	79	114	79	28	79	31	79	24
80	97	80	107	80	91	80	98	80	102	80	33	80	30	80	33
81	92	81	105	81	92	81	70	81	81	81	38	81	31	81	32
82	92	82	120	82	84	82	75	82	74	82	24	82	35	82	33
83	87	83	91	83	103	83	73	83	74	83	26	83	32	83	20
84	81	84	97	84	109	84	81	84	55	84	36	84	23	84	19
85	92	85	96	85	84	85	57	85	51	85	20	85	33	85	20
86	110	86	82	86	86	86	70	86	41	86	35	86	25	86	27
87	95	87	92	87	82	87	74	87	49	87	28	87	35	87	27
88	98	88	101	88	92	88	72	88	40	88	29	88	18	88	27
89	100	89	91	89	71	89	78	89	49	89	39	89	33	89	28
90	83	90	126	90	103	90	66	90	43	90	41	90	23	90	33
91	92	91	103	91	104	91	88	91	57	91	29	91	24	91	28
92	88	92	100	92	108	92	94	92	42	92	29	92	31	92	16
93	76	93	82	93	85	93	70	93	44	93	32	93	26	93	26
94	71	94	81	94	98	94	109	94	54	94	24	94	29	94	20
95	64	95	83	95	105	95	106	95	50	95	31	95	30	95	25
96	70	96	89	96	95	96	88	96	54	96	27	96	21	96	35
97	55	97	80	97	77	97	98	97	54	97	33	97	33	97	31
98	52	98	93	98	94	98	111	98	52	98	29	98	22	98	29
99	61	99	83	99	73	99	85	99	60	99	28	99	31	99	39
100	51	100	66	100	74	100	83	100	57	100	53	100	29	100	28
101	53	101	61	101	61	101	82	101	55	101	38	101	28	101	38
102	37	102	64	102	67	102	72	102	45	102	37	102	25	102	40
103	31	103	44	103	58	103	74	103	44	103	36	103	40	103	43
104	22	104	50	104	51	104	65	104	39	104	31	104	45	104	25
105	22	105	46	105	54	105	58	105	28	105	30	105	42	105	16
106	22	106	35	106	45	106	51	106	21	106	24	106	25	106	15
107	22	107	39	107	45	107	27	107	19	107	21	107	25	107	13
108	17	108	24	108	42	108	29	108	12	108	14	108	16	108	14
109	16	109	20	109	41	109	23	109	13	109	11	109	19	109	15
110	17	110	22	110	30	110	21	110	7	110	11	110	14	110	10
111	15	111	16	111	28	111	18	111	9	111	7	111	12	111	7
112	13	112	23	112	18	112	14	112	10	112	5	112	9	112	11
113	10	113	11	113	21	113	18	113	3	113	6	113	10	113	6
114	16	114	23	114	21	114	8	114	9	114	10	114	7	114	10
115	16	115	20	115	15	115	14	115	4	115	6	115	8	115	7
116	17	116	23	116	17	116	11	116	2	116	3	116	9	116	2
117	19	117	14	117	18	117	11	117	6	117	3	117	9	117	1
118	17	118	17	118	21	118	9	118	6	118	2	118	6	119	2
119	18	119	20	119	16	119	12	119	3	119	5	119	5	122	1
120	8	120	21	120	17	120	9	120	2	120	3	120	5		
121	9	121	7	121	16	121	8	122	1	122	1	121	7		
122	17	122	21	122	10	122	11	127	1	123	2	122	1		
123	14	123	15	123	13	123	6	128	1	124	2	123	2		
124	10	124	17	124	16	124	9			125	1				
125	9	125	10	125	15	125	8			133	1				
126	9	126	13	126	11	126	6								
127	4	127	13	127	12	127	4								
128	11	128	9	128	9	128	3								
129	8	129	15	129	6	129	3								
130	4	130	12	130	9	130	4								
131	2	131	12	131	5	131	1								
132	5	132	7	132	9	132	2								
133	1	133	10	133	2	136	1								
134	1	134	9	134	6	139	1								
135	1	135	9	135	8										

Sample 7, load analysis data. Pictures in black and white. Arcada, 2018

sample 7, 3.6 N		sample 7, 17.85 N		sample 7, 24.97 N		sample 7, 39.23 N		sample 7, 52.74 N		sample 7, 67 N		sample 7, 74.12 N		sample 7, 88.38 N	
0	217806	0	240040	0	247219	0	235566	0	228640	0	236528	0	242783	0	256458
1	9919	1	9522	1	9156	1	10861	1	11254	1	11143	1	12098	1	10923
2	5493	2	5095	2	4219	2	5397	2	5911	2	5777	2	5945	2	5631
3	4239	3	3566	3	3035	3	3945	3	4282	3	3989	3	4118	3	3933
4	3480	4	2797	4	2445	4	3271	4	3422	4	3262	4	3109	4	2934
5	2932	5	2255	5	2127	5	2809	5	2786	5	2617	5	2607	5	2344
6	2672	6	2014	6	1823	6	2341	6	2476	6	2313	6	2252	6	1935
7	2396	7	1782	7	1628	7	2217	7	2248	7	2005	7	1944	7	1746
8	2387	8	1714	8	1475	8	1951	8	1904	8	1872	8	1699	8	1500
9	2133	9	1493	9	1409	9	1721	9	1799	9	1767	9	1661	9	1351
10	1994	10	1347	10	1269	10	1461	10	1685	10	1628	10	1484	10	1186
11	1943	11	1298	11	1165	11	1445	11	1670	11	1531	11	1393	11	1050
12	1922	12	1217	12	1076	12	1308	12	1517	12	1426	12	1392	12	873
13	1668	13	1160	13	1070	13	1174	13	1453	13	1476	13	1244	13	751
14	1589	14	1006	14	977	14	1077	14	1438	14	1335	14	1209	14	712
15	1632	15	987	15	882	15	961	15	1317	15	1300	15	1186	15	634
16	1476	16	954	16	882	16	933	16	1270	16	1286	16	1102	16	638
17	1422	17	918	17	761	17	834	17	1260	17	1137	17	1083	17	590
18	1310	18	814	18	715	18	847	18	1193	18	1163	18	990	18	522
19	1267	19	800	19	666	19	837	19	1140	19	1123	19	1001	19	482
20	1207	20	794	20	554	20	747	20	1076	20	1138	20	902	20	442
21	1132	21	786	21	636	21	727	21	1072	21	1077	21	856	21	469
22	1040	22	742	22	583	22	694	22	1015	22	1081	22	794	22	397
23	1068	23	713	23	550	23	694	23	1027	23	1031	23	759	23	428
24	972	24	682	24	522	24	665	24	942	24	928	24	713	24	379
25	991	25	680	25	505	25	619	25	944	25	915	25	686	25	366
26	960	26	577	26	490	26	606	26	925	26	912	26	650	26	333
27	927	27	579	27	487	27	597	27	934	27	791	27	561	27	341
28	896	28	593	28	453	28	606	28	902	28	763	28	556	28	331
29	902	29	509	29	432	29	573	29	862	29	710	29	486	29	299
30	902	30	530	30	436	30	517	30	767	30	667	30	411	30	283
31	831	31	476	31	435	31	516	31	862	31	628	31	434	31	251
32	779	32	458	32	399	32	488	32	777	32	625	32	400	32	251
33	761	33	437	33	384	33	462	33	741	33	571	33	340	33	242
34	804	34	426	34	331	34	455	34	708	34	519	34	322	34	251
35	695	35	456	35	348	35	434	35	634	35	504	35	296	35	242
36	647	36	397	36	363	36	459	36	616	36	484	36	298	36	222
37	654	37	421	37	382	37	418	37	618	37	449	37	290	37	231
38	649	38	410	38	351	38	377	38	597	38	388	38	300	38	215
39	625	39	381	39	352	39	420	39	538	39	344	39	243	39	205
40	548	40	331	40	333	40	386	40	457	40	306	40	277	40	202
41	583	41	351	41	302	41	378	41	463	41	251	41	247	41	190
42	559	42	357	42	319	42	353	42	426	42	252	42	237	42	150
43	510	43	336	43	295	43	351	43	427	43	210	43	227	43	159
44	477	44	316	44	302	44	335	44	398	44	215	44	212	44	159
45	524	45	316	45	275	45	324	45	366	45	200	45	206	45	153
46	435	46	305	46	268	46	368	46	288	46	205	46	162	46	132
47	469	47	317	47	253	47	305	47	282	47	208	47	173	47	126
48	410	48	290	48	259	48	287	48	301	48	171	48	191	48	114
49	405	49	324	49	217	49	327	49	245	49	165	49	149	49	127
50	377	50	278	50	255	50	294	50	226	50	169	50	170	50	119
51	406	51	265	51	208	51	294	51	228	51	174	51	162	51	115
52	364	52	247	52	226	52	286	52	231	52	176	52	126	52	104
53	377	53	235	53	227	53	263	53	214	53	162	53	137	53	79
54	351	54	244	54	231	54	284	54	234	54	154	54	162	54	99

55	318	55	238	55	191	55	272	55	210	55	130	55	131	55	80
56	356	56	240	56	254	56	267	56	202	56	137	56	141	56	57
57	346	57	234	57	231	57	288	57	203	57	149	57	135	57	80
58	344	58	238	58	215	58	299	58	185	58	144	58	161	58	67
59	374	59	218	59	247	59	269	59	180	59	163	59	160	59	81
60	361	60	236	60	233	60	321	60	174	60	161	60	158	60	69
61	390	61	224	61	281	61	345	61	189	61	132	61	153	61	64
62	389	62	251	62	291	62	329	62	169	62	128	62	122	62	70
63	381	63	263	63	333	63	327	63	198	63	150	63	128	63	55
64	387	64	265	64	320	64	301	64	194	64	148	64	135	64	72
65	360	65	284	65	320	65	302	65	183	65	122	65	130	65	65
66	359	66	275	66	297	66	255	66	155	66	127	66	88	66	69
67	338	67	293	67	314	67	259	67	170	67	130	67	92	67	75
68	338	68	268	68	283	68	224	68	136	68	105	68	87	68	83
69	297	69	295	69	282	69	190	69	147	69	124	69	83	69	69
70	286	70	344	70	214	70	174	70	148	70	94	70	74	70	57
71	325	71	332	71	196	71	168	71	113	71	111	71	62	71	51
72	286	72	275	72	184	72	153	72	114	72	94	72	55	72	59
73	269	73	240	73	193	73	147	73	101	73	100	73	59	73	44
74	252	74	220	74	157	74	143	74	111	74	107	74	38	74	30
75	244	75	192	75	158	75	177	75	97	75	98	75	39	75	42
76	254	76	153	76	149	76	148	76	90	76	114	76	41	76	42
77	233	77	163	77	134	77	152	77	95	77	122	77	33	77	27
78	230	78	143	78	125	78	117	78	102	78	110	78	31	78	30
79	213	79	141	79	124	79	131	79	87	79	103	79	24	79	30
80	216	80	148	80	146	80	123	80	85	80	98	80	25	80	20
81	187	81	159	81	132	81	143	81	62	81	79	81	41	81	21
82	216	82	116	82	92	82	120	82	87	82	83	82	28	82	27
83	200	83	135	83	103	83	113	83	86	83	63	83	29	83	30
84	151	84	127	84	128	84	99	84	78	84	70	84	26	84	33
85	145	85	121	85	101	85	112	85	77	85	59	85	28	85	26
86	153	86	109	86	109	86	102	86	84	86	55	86	26	86	24
87	144	87	105	87	102	87	100	87	83	87	60	87	25	87	20
88	134	88	134	88	113	88	84	88	80	88	36	88	42	88	33
89	124	89	109	89	109	89	107	89	77	89	53	89	30	89	27
90	146	90	132	90	106	90	89	90	69	90	42	90	24	90	29
91	148	91	109	91	116	91	97	91	83	91	42	91	30	91	21
92	127	92	110	92	110	92	101	92	91	92	38	92	26	92	33
93	133	93	106	93	107	93	85	93	98	93	41	93	33	93	26
94	132	94	117	94	99	94	103	94	85	94	39	94	42	94	35
95	121	95	102	95	100	95	104	95	104	95	56	95	32	95	28
96	115	96	90	96	101	96	102	96	81	96	53	96	40	96	31
97	118	97	105	97	103	97	93	97	87	97	43	97	30	97	32
98	102	98	94	98	102	98	109	98	96	98	43	98	32	98	34
99	104	99	106	99	105	99	86	99	83	99	37	99	28	99	27
100	86	100	86	100	94	100	102	100	89	100	37	100	29	100	32
101	86	101	100	101	92	101	94	101	86	101	32	101	36	101	38
102	102	102	114	102	91	102	93	102	85	102	29	102	26	102	29
103	96	103	84	103	107	103	103	103	80	103	36	103	32	103	33
104	86	104	98	104	100	104	101	104	99	104	38	104	35	104	32
105	88	105	87	105	98	105	106	105	101	105	45	105	40	105	30
106	76	106	109	106	90	106	89	106	82	106	45	106	30	106	32
107	98	107	98	107	88	107	109	107	70	107	43	107	32	107	32
108	67	108	75	108	88	108	75	108	77	108	39	108	25	108	25
109	75	109	96	109	97	109	83	109	73	109	31	109	39	109	39
110	82	110	88	110	74	110	99	110	67	110	38	110	37	110	37

111	91	111	77	111	76	111	93	111	65	111	29	111	35	111	26
112	91	112	67	112	54	112	80	112	86	112	33	112	34	112	24
113	77	113	72	113	54	113	80	113	71	113	20	113	29	113	21
114	71	114	82	114	63	114	82	114	52	114	17	114	27	114	24
115	76	115	57	115	58	115	58	115	51	115	23	115	34	115	28
116	48	116	78	116	45	116	61	116	58	116	23	116	25	116	24
117	54	117	61	117	54	117	71	117	58	117	25	117	28	117	17
118	59	118	48	118	54	118	56	118	53	118	18	118	18	118	22
119	51	119	44	119	32	119	47	119	38	119	26	119	20	119	15
120	54	120	40	120	41	120	32	120	42	120	21	120	14	120	16
121	48	121	44	121	41	121	51	121	30	121	18	121	26	121	14
122	42	122	40	122	29	122	55	122	36	122	23	122	14	122	11
123	42	123	20	123	20	123	38	123	23	123	21	123	7	123	11
124	43	124	25	124	21	124	38	124	34	124	15	124	11	124	14
125	54	125	26	125	20	125	44	125	29	125	9	125	18	125	14
126	36	126	28	126	18	126	37	126	32	126	13	126	11	126	11
127	29	127	22	127	22	127	38	127	24	127	12	127	12	127	15
128	20	128	26	128	27	128	40	128	22	128	6	128	15	128	14
129	21	129	19	129	31	129	41	129	19	129	9	129	9	129	14
130	26	130	22	130	21	130	37	130	11	130	6	130	10	130	9
131	27	131	28	131	28	131	38	131	9	131	4	131	5	131	10
132	24	132	25	132	34	132	31	132	3	132	1	132	10	132	18
133	39	133	21	133	27	133	22	133	3	133	1	133	3	133	14
134	22	134	18	134	20	134	23	134	2			134	5	134	8
135	24	135	31	135	24	135	30	135	1			135	3	135	4
136	22	136	16	136	29	136	20	136	1			136	2	136	2
137	22	137	14	137	29	137	19	137	1			137	2	137	8
138	26	138	28	138	32	138	16							138	1
139	16	139	18	139	26	139	14							139	1
140	17	140	31	140	24	140	13							140	3
141	15	141	27	141	21	141	17							142	1
142	16	142	20	142	22	142	13							143	1
143	14	143	29	143	22	143	15							144	1
144	19	144	13	144	28	144	11							145	1
145	24	145	20	145	9	145	16								
146	13	146	20	146	17	146	15								
147	15	147	15	147	14	147	13								
148	17	148	14	148	15	148	12								
149	16	149	23	149	9	149	2								
150	18	150	25	150	14	150	12								
151	7	151	12	151	10	151	4								
152	10	152	11	152	7	152	2								
153	8	153	19	153	10	153	7								
154	6	154	12	154	16	154	3								
155	8	155	9	155	10	155	1								
156	3	156	13	156	5	156	2								
157	4	157	9	157	10	157	1								
158	3	158	12	158	5										
159	4	159	7	159	2										
160	1	160	5	160	3										
165	1	161	9	161	4										
166	1	162	2	162	1										

Sample 8, load analysis data. Pictures in black and white. Arcada, 2018

sampe 8, 3.6 N		sample 8, 17.85 N		sample 8, 24.97 N		sample 8, 39.23 N		sample 8, 52.74 N		sample 8, 67 N		sample 8, 74.12 N		sample 8, 88.38 N
0	230304	0	232623	0	229451	0	234478	0	226939	0	235158	0	232309	0
1	12776	1	11790	1	12336	1	9191	1	10014	1	10335	1	10744	1
2	6457	2	7167	2	6437	2	5990	2	6490	2	4917	2	5408	2
3	4882	3	5227	3	4658	3	4736	3	4854	3	3641	3	3884	3
4	3673	4	4054	4	3848	4	3810	4	3997	4	2869	4	3075	4
5	3247	5	3210	5	3235	5	3270	5	3315	5	2519	5	2584	5
6	2688	6	2743	6	2952	6	2744	6	2852	6	2201	6	2337	6
7	2454	7	2276	7	2687	7	2394	7	2572	7	2043	7	2264	7
8	2238	8	2014	8	2448	8	2122	8	2334	8	1827	8	2067	8
9	1985	9	1795	9	2265	9	1977	9	2068	9	1669	9	1685	9
10	1938	10	1641	10	2064	10	1767	10	1921	10	1528	10	1588	10
11	1739	11	1501	11	1912	11	1678	11	1701	11	1398	11	1416	11
12	1721	12	1436	12	1670	12	1454	12	1614	12	1309	12	1339	12
13	1621	13	1310	13	1549	13	1339	13	1388	13	1229	13	1199	13
14	1567	14	1170	14	1266	14	1261	14	1310	14	1158	14	1165	14
15	1459	15	1146	15	1210	15	1195	15	1207	15	1114	15	1129	15
16	1271	16	1078	16	1073	16	1146	16	1115	16	1022	16	991	16
17	1168	17	1026	17	975	17	1023	17	1068	17	987	17	958	17
18	1102	18	1049	18	962	18	970	18	1012	18	891	18	938	18
19	950	19	897	19	847	19	887	19	956	19	784	19	826	19
20	855	20	882	20	806	20	830	20	914	20	785	20	838	20
21	808	21	866	21	822	21	851	21	831	21	726	21	820	21
22	743	22	809	22	770	22	745	22	785	22	693	22	730	22
23	649	23	744	23	757	23	742	23	710	23	682	23	711	23
24	564	24	758	24	759	24	650	24	720	24	638	24	659	24
25	537	25	725	25	712	25	648	25	631	25	640	25	617	25
26	528	26	636	26	710	26	586	26	653	26	583	26	612	26
27	501	27	590	27	656	27	513	27	614	27	540	27	550	27
28	449	28	580	28	656	28	514	28	600	28	555	28	554	28
29	414	29	538	29	547	29	518	29	576	29	545	29	574	29
30	468	30	545	30	578	30	493	30	580	30	556	30	540	30
31	452	31	517	31	536	31	491	31	550	31	476	31	510	31
32	380	32	497	32	513	32	492	32	535	32	478	32	490	32
33	373	33	505	33	498	33	409	33	497	33	469	33	526	33
34	392	34	459	34	407	34	438	34	506	34	480	34	471	34
35	363	35	477	35	416	35	430	35	489	35	477	35	417	35
36	371	36	414	36	395	36	424	36	407	36	443	36	432	36
37	324	37	395	37	364	37	392	37	459	37	463	37	373	37
38	309	38	411	38	378	38	411	38	413	38	439	38	426	38
39	305	39	405	39	301	39	415	39	440	39	447	39	406	39
40	301	40	329	40	343	40	370	40	451	40	424	40	412	40
41	300	41	330	41	305	41	379	41	426	41	437	41	384	41
42	273	42	294	42	315	42	335	42	425	42	443	42	362	42
43	261	43	275	43	294	43	367	43	386	43	414	43	390	43
44	223	44	252	44	293	44	327	44	407	44	372	44	337	44
45	232	45	271	45	293	45	337	45	381	45	427	45	333	45
46	201	46	255	46	305	46	353	46	421	46	381	46	316	46
47	205	47	214	47	271	47	312	47	372	47	365	47	330	47
48	211	48	235	48	276	48	307	48	374	48	353	48	292	48
49	182	49	213	49	280	49	323	49	398	49	338	49	328	49

50	201	50	241	50	293	50	298	50	388	50	342	50	309	50	256
51	176	51	234	51	280	51	302	51	399	51	317	51	271	51	225
52	187	52	230	52	286	52	292	52	402	52	318	52	282	52	257
53	173	53	202	53	280	53	313	53	399	53	287	53	291	53	261
54	178	54	206	54	263	54	276	54	368	54	303	54	306	54	225
55	198	55	219	55	251	55	294	55	385	55	284	55	299	55	229
56	208	56	221	56	289	56	266	56	379	56	311	56	252	56	242
57	234	57	213	57	282	57	248	57	402	57	287	57	255	57	251
58	205	58	202	58	237	58	270	58	396	58	306	58	248	58	266
59	200	59	211	59	268	59	268	59	393	59	308	59	314	59	247
60	208	60	192	60	256	60	339	60	368	60	276	60	268	60	272
61	217	61	196	61	277	61	284	61	391	61	266	61	276	61	268
62	199	62	231	62	239	62	318	62	363	62	282	62	276	62	270
63	213	63	224	63	269	63	325	63	370	63	294	63	273	63	288
64	265	64	259	64	255	64	301	64	391	64	322	64	297	64	300
65	244	65	222	65	293	65	292	65	372	65	286	65	232	65	294
66	239	66	240	66	266	66	295	66	336	66	287	66	265	66	276
67	261	67	232	67	261	67	254	67	349	67	300	67	212	67	277
68	256	68	182	68	278	68	224	68	337	68	275	68	223	68	252
69	260	69	206	69	227	69	212	69	307	69	278	69	213	69	269
70	232	70	184	70	225	70	220	70	287	70	259	70	223	70	230
71	222	71	198	71	214	71	207	71	220	71	251	71	224	71	239
72	222	72	179	72	220	72	197	72	234	72	247	72	221	72	242
73	188	73	137	73	195	73	184	73	225	73	224	73	222	73	198
74	206	74	151	74	163	74	177	74	197	74	198	74	205	74	230
75	221	75	130	75	156	75	175	75	190	75	232	75	200	75	187
76	190	76	101	76	145	76	169	76	159	76	236	76	208	76	207
77	199	77	118	77	145	77	166	77	155	77	229	77	237	77	215
78	177	78	101	78	124	78	166	78	139	78	213	78	221	78	227
79	175	79	95	79	108	79	133	79	168	79	214	79	184	79	196
80	146	80	98	80	130	80	143	80	156	80	186	80	218	80	203
81	168	81	84	81	104	81	131	81	171	81	210	81	201	81	195
82	143	82	105	82	102	82	103	82	166	82	195	82	186	82	221
83	142	83	84	83	62	83	129	83	148	83	175	83	218	83	174
84	158	84	96	84	66	84	124	84	125	84	171	84	164	84	168
85	140	85	74	85	71	85	100	85	147	85	187	85	193	85	192
86	142	86	60	86	71	86	120	86	129	86	188	86	201	86	174
87	157	87	61	87	65	87	122	87	113	87	157	87	204	87	208
88	155	88	54	88	45	88	102	88	127	88	150	88	195	88	211
89	131	89	50	89	45	89	70	89	90	89	153	89	167	89	204
90	121	90	43	90	44	90	42	90	104	90	165	90	213	90	187
91	92	91	34	91	42	91	39	91	89	91	146	91	197	91	189
92	92	92	35	92	40	92	45	92	105	92	138	92	206	92	222
93	76	93	43	93	37	93	47	93	84	93	156	93	198	93	227
94	88	94	30	94	43	94	46	94	86	94	128	94	162	94	215
95	90	95	31	95	29	95	39	95	72	95	147	95	191	95	234
96	85	96	26	96	42	96	24	96	76	96	139	96	141	96	266
97	76	97	32	97	26	97	21	97	73	97	163	97	187	97	241
98	79	98	28	98	26	98	21	98	57	98	126	98	155	98	245
99	73	99	31	99	23	99	22	99	86	99	130	99	163	99	244
100	78	100	24	100	21	100	17	100	59	100	138	100	165	100	235

101	54	101	34	101	15	101	14	101	61	101	128	101	156	101	175
102	59	102	25	102	29	102	20	102	57	102	108	102	148	102	187
103	45	103	17	103	21	103	27	103	53	103	108	103	129	103	163
104	36	104	17	104	22	104	13	104	73	104	121	104	137	104	178
105	44	105	21	105	13	105	13	105	50	105	112	105	157	105	145
106	24	106	18	106	13	106	13	106	49	106	118	106	128	106	134
107	27	107	13	107	27	107	14	107	41	107	108	107	141	107	144
108	21	108	21	108	14	108	10	108	35	108	99	108	151	108	132
109	18	109	21	109	13	109	19	109	44	109	95	109	123	109	119
110	24	110	20	110	18	110	10	110	27	110	101	110	127	110	132
111	21	111	28	111	16	111	14	111	25	111	64	111	105	111	140
112	15	112	21	112	15	112	16	112	25	112	79	112	124	112	139
113	20	113	29	113	12	113	15	113	21	113	70	113	113	113	120
114	13	114	30	114	10	114	18	114	22	114	69	114	125	114	113
115	22	115	14	115	12	115	7	115	17	115	69	115	129	115	144
116	22	116	15	116	19	116	18	116	26	116	56	116	99	116	141
117	19	117	18	117	14	117	10	117	15	117	43	117	93	117	136
118	7	118	19	118	19	118	13	118	15	118	40	118	104	118	136
119	27	119	10	119	15	119	12	119	14	119	50	119	89	119	121
120	15	120	12	120	19	120	10	120	20	120	65	120	109	120	125
121	19	121	17	121	18	121	8	121	16	121	45	121	90	121	110
122	23	122	18	122	19	122	17	122	19	122	44	122	77	122	90
123	22	123	17	123	25	123	17	123	18	123	38	123	63	123	65
124	18	124	16	124	19	124	15	124	15	124	26	124	53	124	57
125	26	125	18	125	27	125	14	125	12	125	24	125	51	125	49
126	23	126	27	126	18	126	12	126	5	126	18	126	43	126	37
127	26	127	19	127	26	127	9	127	8	127	9	127	42	127	51
128	23	128	22	128	21	128	5	128	2	128	6	128	42	128	22
129	21	129	17	129	13	129	6	129	2	129	9	129	40	129	42
130	12	130	24	130	17	130	1	130	2	130	10	130	32	130	45
131	16	131	21	131	10	131	2	131	1	131	6	131	17	131	43
132	24	132	18	132	13	132	1			132	5	132	13	132	41
133	15	133	25	133	4	133	1			133	2	133	6	133	40
134	15	134	7	134	6					134	3	134	6	134	28
135	17	135	8	135	4					137	1	135	5	135	30
136	13	136	6	136	9					140	3	136	10	136	24
137	15	137	6	137	2							137	10	137	18
138	15	138	8	138	10							138	10	138	19
139	13	139	7	139	7							139	2	139	9
140	11	140	5	140	5							140	6	140	9
141	17	141	7	141	5							141	6	141	6
142	5	142	4	142	1							142	2	142	9
143	17	143	8	143	3							143	1	143	4
144	14	144	5	145	2							144	3	144	3
145	9	145	4									145	1	145	4
146	12	146	3									149	2	146	1
147	7	147	2									150	2	147	2
148	10	148	2											148	1
149	6	149	2											151	2
150	1														
151	1														
153	1														

Thermal healing data. Pictures in black and white. Arcada, 2018

sample 2			50°		80°	sample 7			50°		80°	sample 8			50°		80°
0	243719	0	236562	0	294451	0	245911	0	246859	0	299785	0	222740	0	246731	0	303155
1	10704	1	11472	1	4181	1	11097	1	10750	1	2988	1	14004	1	9430	1	1371
2	5048	2	5742	2	2673	2	5129	2	5198	2	1216	2	7918	2	4783	2	673
3	3601	3	4090	3	1891	3	3388	3	3560	3	825	3	5314	3	3515	3	449
4	2611	4	3250	4	1221	4	2688	4	2877	4	510	4	4137	4	2733	4	282
5	2217	5	2613	5	753	5	2330	5	2383	5	346	5	3147	5	2315	5	197
6	1722	6	2251	6	436	6	2007	6	2044	6	201	6	2528	6	2142	6	106
7	1606	7	2126	7	304	7	1716	7	1784	7	153	7	2165	7	1892	7	99
8	1440	8	1736	8	171	8	1595	8	1484	8	103	8	1967	8	1725	8	79
9	1267	9	1600	9	111	9	1488	9	1341	9	83	9	1752	9	1554	9	91
10	1150	10	1444	10	91	10	1280	10	1244	10	78	10	1625	10	1488	10	60
11	1071	11	1293	11	78	11	1189	11	1126	11	76	11	1488	11	1455	11	85
12	965	12	1199	12	98	12	1110	12	1035	12	79	12	1326	12	1305	12	69
13	924	13	1102	13	89	13	1001	13	924	13	61	13	1239	13	1245	13	56
14	914	14	981	14	80	14	868	14	816	14	57	14	1196	14	1138	14	53
15	825	15	950	15	65	15	876	15	756	15	41	15	1121	15	1083	15	56
16	812	16	827	16	47	16	780	16	691	16	43	16	1111	16	1042	16	46
17	782	17	782	17	56	17	646	17	657	17	40	17	980	17	1046	17	57
18	742	18	776	18	61	18	629	18	647	18	27	18	974	18	943	18	53
19	695	19	721	19	63	19	608	19	614	19	32	19	981	19	950	19	49
20	619	20	725	20	47	20	612	20	539	20	36	20	849	20	941	20	44
21	599	21	696	21	50	21	527	21	535	21	23	21	839	21	843	21	33
22	634	22	673	22	37	22	509	22	532	22	24	22	793	22	809	22	15
23	605	23	659	23	51	23	498	23	505	23	24	23	697	23	831	23	12
24	510	24	667	24	23	24	482	24	522	24	18	24	758	24	694	24	7
25	560	25	583	25	20	25	489	25	463	25	23	25	758	25	750	25	1
26	509	26	559	26	8	26	425	26	447	26	24	26	696	26	695	26	2
27	518	27	527	27	12	27	418	27	445	27	24	27	649	27	618		
28	520	28	557	28	14	28	453	28	425	28	32	28	660	28	637		
29	516	29	554	29	6	29	427	29	387	29	15	29	642	29	563		
30	505	30	531	30	4	30	411	30	419	30	19	30	642	30	525		
31	463	31	506	31	5	31	405	31	395	31	12	31	575	31	460		
32	484	32	492	32	2	32	387	32	371	32	16	32	604	32	464		
33	450	33	492	34	1	33	370	33	380	33	8	33	561	33	406		
34	447	34	437			34	335	34	356	34	19	34	577	34	399		
35	436	35	444			35	356	35	357	35	10	35	551	35	384		
36	423	36	416			36	391	36	305	36	15	36	517	36	309		
37	395	37	441			37	355	37	313	37	11	37	576	37	269		
38	398	38	426			38	325	38	351	38	13	38	535	38	252		
39	367	39	391			39	337	39	297	39	12	39	511	39	240		
40	388	40	402			40	333	40	302	40	1	40	509	40	222		
41	402	41	360			41	289	41	280	41	6	41	498	41	190		
42	335	42	383			42	299	42	264	42	8	42	405	42	186		
43	363	43	362			43	352	43	269	43	3	43	418	43	180		
44	338	44	373			44	321	44	254	44	4	44	443	44	168		
45	345	45	387			45	320	45	264	45	7	45	435	45	170		
46	311	46	391			46	294	46	310	46	5	46	343	46	163		
47	292	47	349			47	308	47	263	47	3	47	366	47	153		
48	323	48	363			48	254	48	269	48	5	48	413	48	165		
49	314	49	345			49	296	49	283	49	5	49	362	49	175		
50	292	50	335			50	319	50	283	50	4	50	346	50	179		
51	349	51	356			51	292	51	306	51	3	51	362	51	163		
52	319	52	349			52	295	52	300	52	3	52	320	52	187		
53	320	53	320			53	311	53	284	53	4	53	302	53	180		
54	311	54	334			54	282	54	298	54	4	54	309	54	200		
55	317	55	357			55	309	55	282	55	2	55	342	55	219		
56	309	56	335			56	301	56	290	56	1	56	313	56	210		
57	308	57	293			57	311	57	242	57	3	57	292	57	208		
58	293	58	306			58	300	58	263	58	2	58	330	58	191		
59	297	59	302			59	283	59	259	59	3	59	340	59	169		
60	317	60	294			60	327	60	264	62	1	60	315	60	189		
61	354	61	299			61	320	61	232	63	1	61	305	61	165		
62	332	62	280			62	319	62	260			62	330	62	183		
63	322	63	292			63	310	63	239			63	295	63	148		
64	332	64	319			64	271	64	217			64	354	64	179		
65	319	65	291			65	269	65	236			65	327	65	160		
66	312	66	269			66	244	66	210			66	371	66	170		
67	321	67	292			67	221	67	217			67	368	67	185		

68	282	68	265			68	220	68	209			68	344	68	194
69	292	69	264			69	198	69	208			69	330	69	193
70	235	70	238			70	164	70	196			70	308	70	206
71	232	71	236			71	163	71	170			71	320	71	151
72	209	72	228			72	162	72	192			72	287	72	149
73	206	73	206			73	162	73	180			73	268	73	146
74	182	74	179			74	126	74	189			74	232	74	108
75	183	75	170			75	146	75	174			75	242	75	128
76	169	76	153			76	125	76	111			76	232	76	127
77	140	77	166			77	130	77	151			77	223	77	92
78	160	78	174			78	116	78	117			78	204	78	100
79	161	79	179			79	100	79	129			79	181	79	89
80	151	80	131			80	119	80	120			80	188	80	101
81	167	81	145			81	112	81	110			81	182	81	82
82	134	82	130			82	110	82	130			82	160	82	63
83	118	83	131			83	98	83	122			83	161	83	78
84	109	84	110			84	100	84	115			84	151	84	72
85	111	85	117			85	105	85	109			85	170	85	48
86	95	86	107			86	107	86	116			86	133	86	38
87	85	87	106			87	107	87	118			87	130	87	48
88	86	88	106			88	103	88	106			88	134	88	34
89	108	89	93			89	109	89	82			89	116	89	41
90	73	90	88			90	102	90	89			90	86	90	26
91	91	91	101			91	91	91	109			91	85	91	29
92	65	92	112			92	91	92	90			92	87	92	23
93	72	93	98			93	93	93	92			93	88	93	21
94	76	94	94			94	93	94	97			94	83	94	21
95	60	95	111			95	91	95	91			95	96	95	19
96	62	96	85			96	67	96	97			96	84	96	15
97	81	97	96			97	61	97	81			97	90	97	10
98	83	98	89			98	60	98	71			98	74	98	13
99	72	99	84			99	54	99	68			99	84	99	8
100	82	100	104			100	48	100	74			100	77	100	6
101	57	101	62			101	54	101	63			101	61	101	7
102	56	102	68			102	60	102	78			102	46	102	5
103	53	103	73			103	37	103	49			103	51	103	5
104	48	104	61			104	30	104	42			104	56	104	5
105	62	105	61			105	31	105	45			105	38	105	4
106	52	106	38			106	20	106	60			106	45	106	5
107	38	107	52			107	16	107	41			107	53	107	6
108	50	108	50			108	11	108	34			108	56	108	5
109	40	109	38			109	2	109	38			109	51	109	4
110	43	110	38			110	5	110	24			110	38	110	2
111	30	111	36			138	1	111	17			111	32	111	4
112	34	112	28			140	1	112	11			112	37	112	5
113	38	113	44			144	1	113	7			113	32	113	2
114	32	114	28					114	1			114	24	114	1
115	28	115	32					122	1			115	22		
116	32	116	29					124	1			116	15		
117	33	117	31					132	1			117	17		
118	22	118	20									118	18		
119	22	119	14									119	15		
120	16	120	13									120	11		
121	12	121	11									121	6		
122	13	122	7									122	8		
123	14	123	3									123	5		
124	10	124	8									124	3		
125	11	125	5									125	3		
126	6	126	1									126	5		
127	1	127	2									127	3		
128	5	128	3									136	1		
129	1	129	5									137	1		
130	1	130	4									143	1		
		131	3												
		133	1												
		134	2												
		138	1												
		141	1												